EurJOC European Journal of Organic Chemistry

FULL PAPER

DOI: 10.1002/ejoc.201301006

Synthesis and Properties of Azulene-Substituted Donor–Acceptor Chromophores Connected by Arylamine Cores

Taku Shoji,*[a] Erika Shimomura,[a] Mitsuhisa Maruyama,[a] Akifumi Maruyama,[a] Shunji Ito,[b] Tetsuo Okujima,[c] Kozo Toyota,[d] and Noboru Morita[d]

Keywords: Arenes / Chromophores / Cycloaddition / Redox chemistry / Cyclic voltammetry

1-Ethynylazulenes connected by several arylamine cores reacted with tetracyanoethylene (TCNE) and 7,7,8,8-tetracyanoquinodimethane (TCNQ) in a formal [2+2] cycloaddition–cycloreversion reaction to afford the corresponding tetracyanobutadiene (TCBD) and dicyanoquinodimethane (DCNQ) chromophores, respectively, in excellent yields. The intramolecular charge-transfer (ICT) characters between the donor (azulene and arylamine cores) and acceptor (TCBD and DCNQ units) moieties were investigated by UV/Vis spectroscopy and theoretical calculations. The redox behavior of the new TCBD and DCNQ derivatives was examined by cyclic voltammetry (CV) and differential pulse voltammetry (DPV), which revealed their multistep electrochemical reduction properties. Moreover, significant color changes were observed by visible spectroscopy under the electrochemical reduction conditions.

Introduction

Arylamine derivatives are very important compounds for the development of organic electronic materials, such as light-emitting diodes (LED),[1] semiconductors,[2] solar cells,[3] memory devices,[4] and others. Donor–acceptor derivatives possessing arylamine moieties have also attracted much interest due to their potential as organic electronics.[5] Therefore, a variety of these derivatives have been synthesized as shown in the literature.

Recently, Diederich et al. reported that a variety of alkynes substituted by arylamine moieties reacted with tetracyanoethylene (TCNE) and 7,7,8,8-tetracyanoquinodimethane (TCNQ) to give tetracyanobutadiene (TCBD) and dicyanoquinodimethane (DCNQ) derivatives, respectively, in excellent yields.[6] They have also reported that the new chromophores obtained by the reaction have potential applications to third-order nonlinear optics, liquid crystals, and molecular batteries. In the meanwhile, Michinobu et al. have reported the synthesis of polymers with multiple TCBD and DCNQ moieties embedded with arylamine units.[7] The polymers with multiple donor–acceptor moieties might become promising candidates with applications to semiconductors in organic photovoltaic devices, nonlinear optical materials, and ion sensors.

We have also reported the synthesis and electrochemical properties of TCBD and DCNQ derivatives with azulenyl,[8] 2-oxo-2*H*-cyclohepta[*b*]-3-furyl,[9] and ferrocenyl[10] substituents, which have been prepared by the [2+2] cycloaddition–cycloreversion reaction of the corresponding acetylene derivatives with TCNE and TCNQ, respectively. Particularly, azulene-substituted TCBDs undergo significant color changes with high reversibility under redox conditions. In addition to azulenyl, 2-oxo-2*H*-cyclohepta[*b*]-3-furyl, and ferrocenyl substituents examined by our groups, arylamino groups also possess strong electron-donating properties and high reactivity. Thus, acetylene derivatives connected by the arylamine cores are expected to be new chromophores with multiple donor–acceptor units by virtue of sequential [2+2] cycloaddition–cycloreversion sequence with TCNE and TCNQ. Furthermore, novel chromophores with multiple donor–acceptor units may exhibit multistage redox behavior due to redox reactions of both donor (i.e., azulene and arylamines) and acceptor moieties.

We describe herein the synthesis of novel azulene-substituted acetylene derivatives connected by several arylamine cores. Molecules of interest are characterized by multiple 1-ethynylazulene units achieved utilizing Sonogashira–Hagihara cross-coupling chemistry, as well as novel TCBD and DCNQ chromophores generated by [2+2] cycloaddition–cycloreversion of azulene-substituted acetylene derivatives with TCNE and TCNQ, respectively. The electronic properties of novel TCBD and DCNQ derivatives

[a] Department of Chemistry, Faculty School of Science, Shinshu University,
Matsumoto 390-8621, Japan
E-mail: tshoji@shinshu-u.ac.jp
http://soar-rd.shinshu-u.ac.jp/profile/en.gmShOakh.html
[b] Graduate School of Science and Technology, Hirosaki University,
Hirosaki 036-8561, Japan
[c] Department of Chemistry and Biology, Graduate School of Science and Engineering, Ehime University,
Matsuyama 790-8577, Japan
[d] Department of Chemistry, Graduate School of Science, Tohoku University,
Sendai 980-8578, Japan

Supporting information for this article is available on the WWW under http://dx.doi.org/10.1002/ejoc.201301006.

connected by the arylamine cores were investigated by absorption spectroscopy, electrochemical analysis and theoretical calculations.

Results and Discussion

Synthesis

The iodide substituent is a very important functional group in the transition-metal-catalyzed cross-coupling reaction of aromatic compounds since aryl iodides possess higher reactivity relative to the corresponding bromides and chlorides.[11] However, difficulty in preparing aryl iodides detracts from their potential applications. Preparation of aromatic iodides is often carried out effectively by using iodination reagents, such as I_2,[12] ICl,[13] and *N*-iodosuccinimide (NIS).[14] However, most such reagents are toxic or expensive, and/or the reaction with the reagents often requires harsh reaction conditions.[12–14] We have recently developed an efficient iodination procedure using NaI in the presence of *N*-chlorosuccinimide (NCS).[8e,9a,15] Thus, we have examined the preparation of iodoarylamines **5**–**8** starting from arylamines **1**–**4**; iodination of **1**–**4** requires that the next reaction be palladium-catalyzed cross-coupling reaction.

Thus, reaction of **1** with NaI/NCS in acetic acid and subsequent chromatographic purification of the reaction mixture on silica gel afforded desired compound **5**[15] in 80% yield (Scheme 1). Likewise, the reaction of **2** and **3** with NaI/NCS afforded the presumed iodination products **6**[16] and **7**[17] in 97% and 71% yields, respectively (Scheme 2 and Scheme 3). Triiodide derivative **8**[18] was also obtained by a similar reaction of **4** with NaI/NCS in 95% yield (Scheme 4). The yields of products in these reactions were comparable to those of reactions with NIS reported in the literatures. Thus, the current procedure has great advantages for the preparation of iodoarylamines, from the perspectives of both product yields and cost-effectiveness.

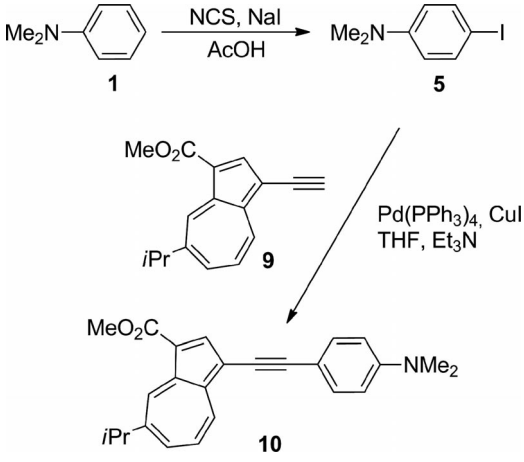

Scheme 1. Synthesis of compound **10**.

Preparation of 1-ethynylazulenes connected by arylamine cores **10**–**14** was accomplished by palladium-catalyzed alkynylation of 1-ethynylazulene **9**[8,19] with corresponding iodoarylamines **5**–**8** under Sonogashira–Hagihara conditions.[20] The cross-coupling reaction of **5** with **9** in the presence of catalytic $Pd(PPh_3)_4$ as in THF/Et_3N at 50 °C afforded methyl 3-(4-dimethylaminophenylethynyl)-7-isopropylazulene-1-carboxylate (**10**) in 99% yield.

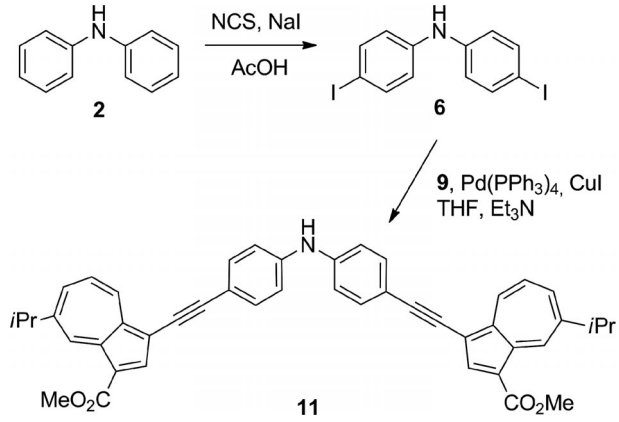

Scheme 2. Synthesis of compound **11**.

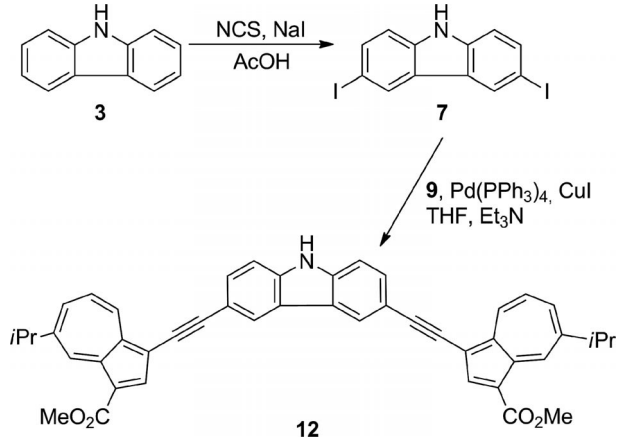

Scheme 3. Synthesis of compound **12**.

Cross-coupling of **6** with **9** using $Pd(PPh_3)_4$ as a catalyst and subsequent chromatographic purification on silica gel afforded desired 4,4′-bis(7-isopropyl-1-methoxycarbonyl-3-azulenylethynyl)diphenylamine (**11**) in 94% yield (Scheme 2). The reaction of **7** with **9** afforded **12** in 85% yield (Scheme 3).

The cross-coupling reaction of **8** with **9** in the presence of catalytic palladium afforded **13** in 90% yield (Scheme 4). These acetylene derivatives **10**–**13** possess fair solubility in common organic solvents ($CHCl_3$, CH_2Cl_2, etc.). Moreover, **10**–**13** are stable showing no decomposition, even after several weeks at room temperature. Consequently, these acetylene derivatives were utilized in further transformations en route to new TCBD and DCNQ derivatives of interest.

The [2+2] cycloaddition–cycloreversion sequence of **10**–**13** with TCNE and TCNQ was applied to generate new TCBD and DCNQ derivatives. The reaction of **10** with TCNE in refluxing EtOAc yielded **14** in 97% yield as the sole product. Alternatively, compounds **15** and **16** were gen-

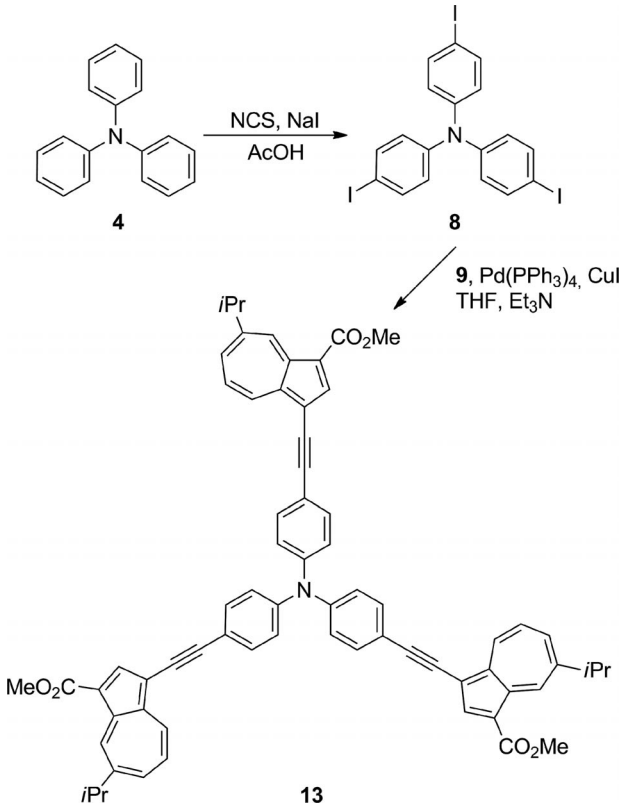

Scheme 4. Synthesis of compound **13**.

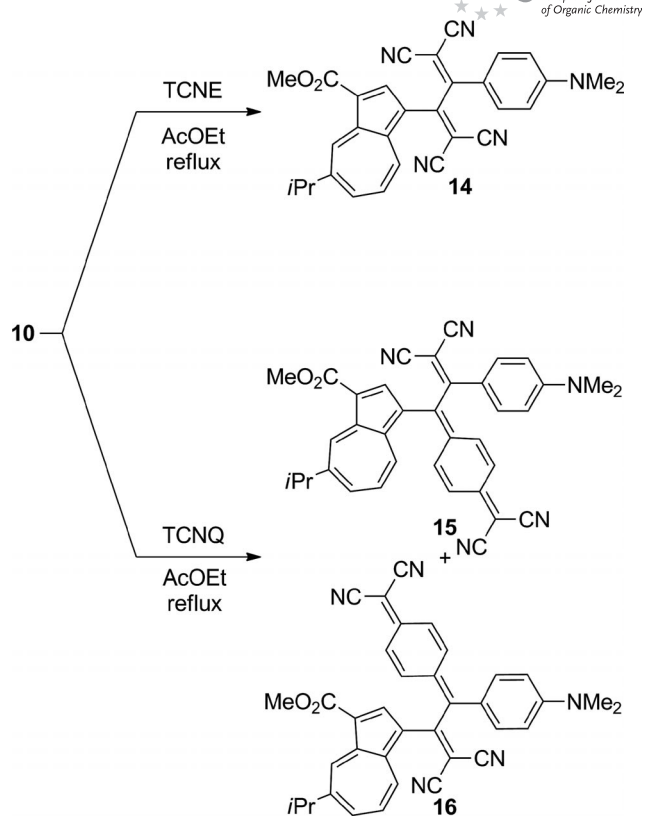

Scheme 5. Reaction of **10** with TCNE and TCNQ.

erated in 43% and 48% yields, respectively, by reaction of **10** with TCNQ (Scheme 5). Recently, Diederich et al. have reported that the regioselectivity of [2+2] cycloadditions of C≡C triple bonds with TCNQ correlates to the electron-donating property of the substituent on the ethynyl group.[21] Thus, the reduced selectivity for generation of **15** and **16** suggests that the 1-azulenyl group in **10** possesses almost the same electron-donating character as that of the *N*,*N*-dimethylanilino (DMA) group.

The double-addition of TCNE to **11** gave **17** in 98% yield after stirring in EtOAc at reflux. DCNQ chromophore **18** was also prepared by one-pot formal [2+2] cycloaddition–cycloreversion reaction of **11** with TCNQ in 91% yield (Scheme 6). The TCBD and DCNQ chromophores, each bearing a carbazole unit, **19** and **20** were obtained in 92% and 84% yields, respectively, by [2+2] cycloaddition–cycloreversion reaction of acetylene precursor **12** with TCNE and TCNQ, respectively (Scheme 7).

Tris adducts **21** and **22** were obtained in excellent yields (**21**: 90%; **22**: 87%) by the cycloaddition reactions of TCNE and TCNQ, respectively, with corresponding alkyne **13** followed by the cycloreversion reaction (Scheme 8). These new

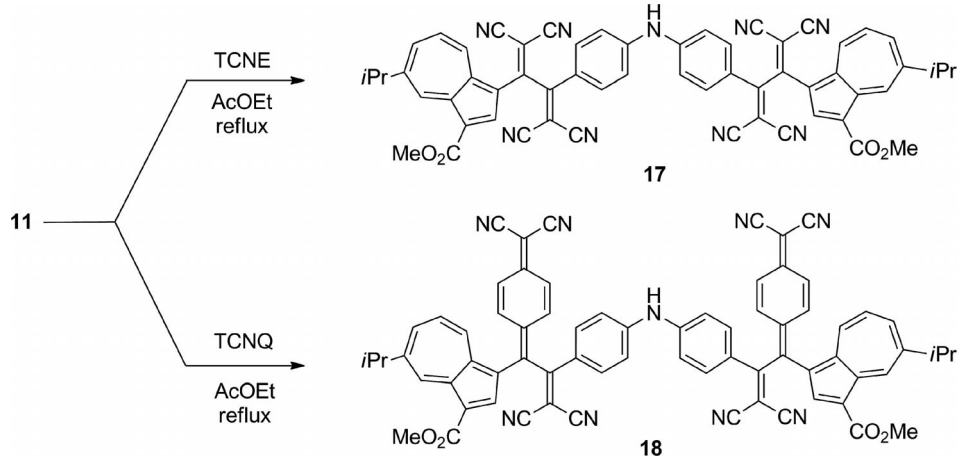

Scheme 6. Reaction of **11** with TCNE and TCNQ.

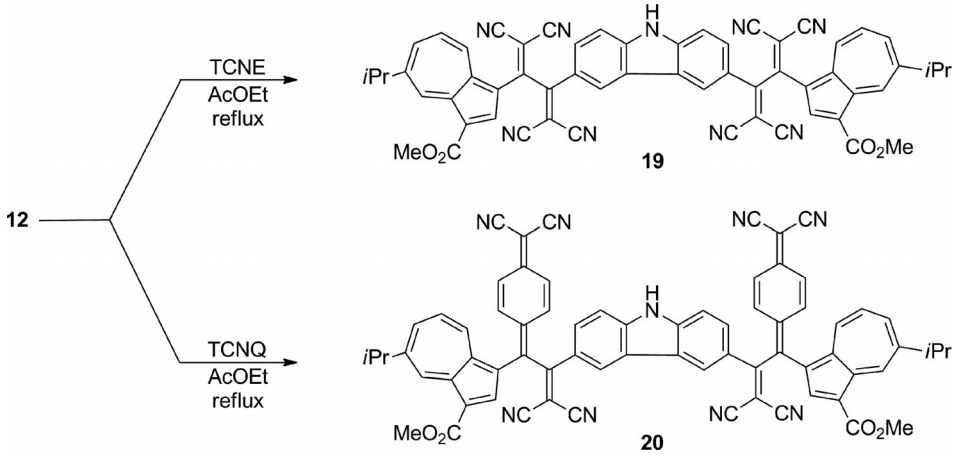

Scheme 7. Reaction of **12** with TCNE and TCNQ.

TCBD and DCNQ derivatives **14**–**22** are obtained as stable crystals and can be easily and reliably stored in the crystalline state under ambient conditions.

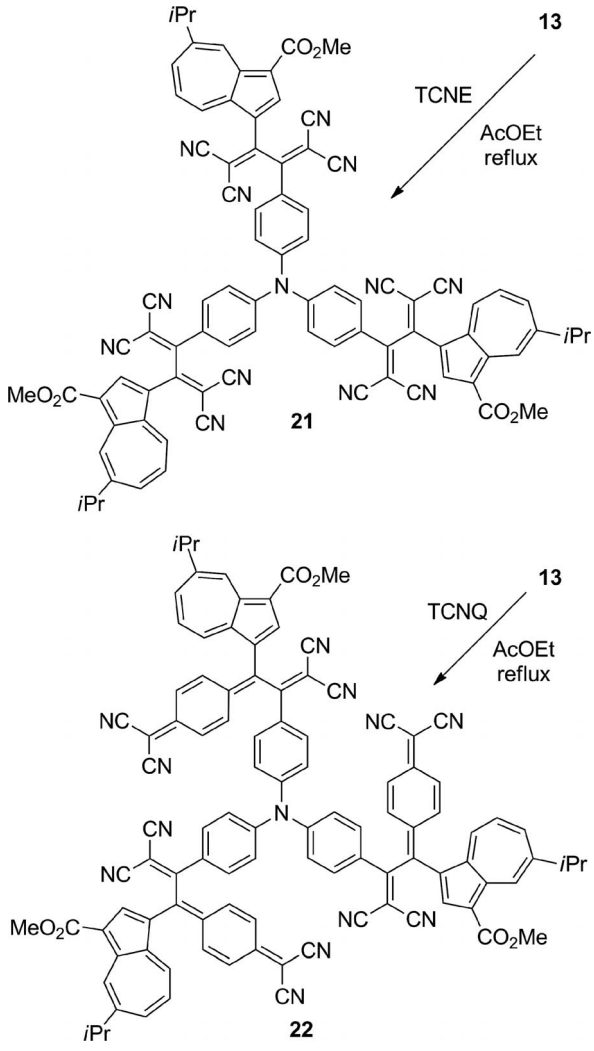

Scheme 8. Reaction of **13** with TCNE and TCNQ.

Properties

New compounds were fully characterized by rigorous analysis of spectroscopic data, as shown in the Supporting Information. Assignment of peaks in the ^{1}H and ^{13}C NMR spectra of the compounds was accomplished by NOE, and COSY, HMQC and HMBC experiments. Mass spectra of **10**–**22** ionized by FAB showed the correct molecular ion peaks. The characteristic stretching vibration band of the acetylene moiety of **10**–**13** was observed at $\tilde{\nu}_{max}$ = 2196–2197 cm^{-1} in their IR spectra. TCBD and DCNQ derivatives **14**–**22** exhibited a characteristic C≡N stretching band at $\tilde{\nu}_{max}$ = 2202–2224 cm^{-1} in their IR spectra. These results are consistent with the structures of the products.

UV/Vis spectra of **10**–**22** are shown in Figures 1, 2, and 3. The absorption maxima and coefficients (logε) of TCBDs and DCNQs **14**–**22** in CH_2Cl_2 and in hexane with certain amounts of CH_2Cl_2 to ensure solubility are summarized in Table 1. The UV/Vis spectra of acetylene derivatives **10**–**13** show characteristic weak absorption bands arising from the azulene system in the visible region. Although extinction coefficients were found to increase with the number of substituted azulene rings, absorption bands in the visible region of these compounds resemble each other (Figure 1). These results suggest that tethering of multiple 1-ethynylazulene moieties with arylamine cores does not allow effective π-conjugation.

TCBD **14** exhibited a broad absorption band at λ_{max} = 474 nm. Likewise, TCBD **17**, with a diphenylamine core, also displayed a broad and strong CT absorption band at λ_{max} = 489 nm. TCBD **21,** with a triphenylamine core, showed a strong absorption band at λ_{max} = 503 nm. The bathochromic shift in the absorption maxima of TCBDs **14**, **17**, and **21**, in accordance with the increase in number of substituted TCBD moieties, suggests π-conjugation of the TCBD moieties with the amine cores as illustrated in Scheme 9. However, absorption maxima of TCBD **19** (λ_{max} = 456 nm) exhibited a hypsochromic shift relative to those of **14**, **17**, and **21**. The absorption maxima of **19** were nearly equal to that of simpler TCBD derivative **23** (λ_{max} =

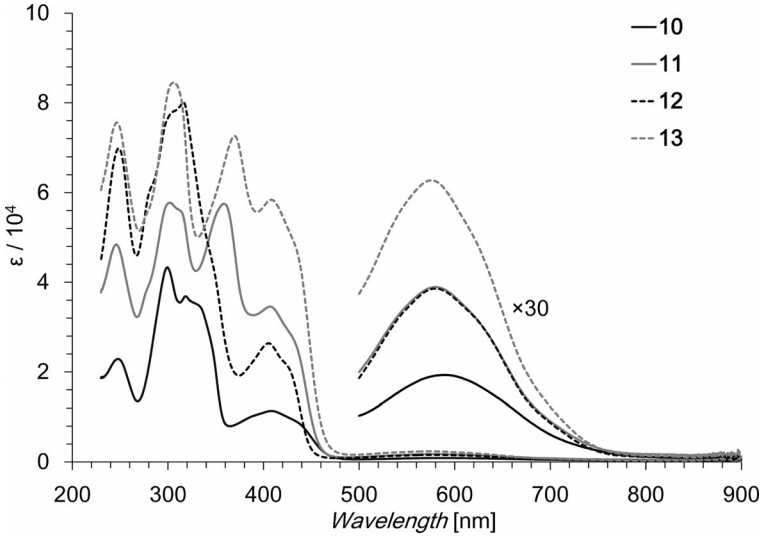

Figure 1. UV/visible spectra of **10** (black line), **11** (gray line), **12** (broken black line), **13** (broken gray line) in CH_2Cl_2.

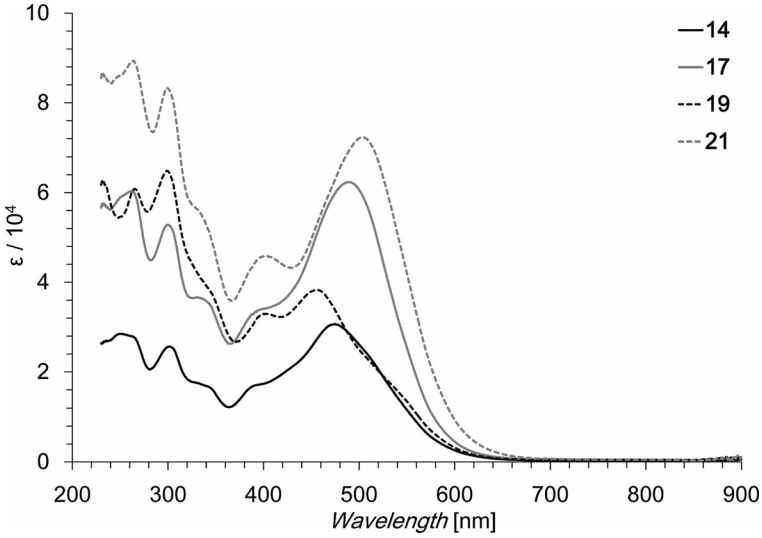

Figure 2. UV/visible spectra of TCBDs **14** (black line), **17** (gray line), **19** (broken black line), and **21** (broken gray line) in CH_2Cl_2.

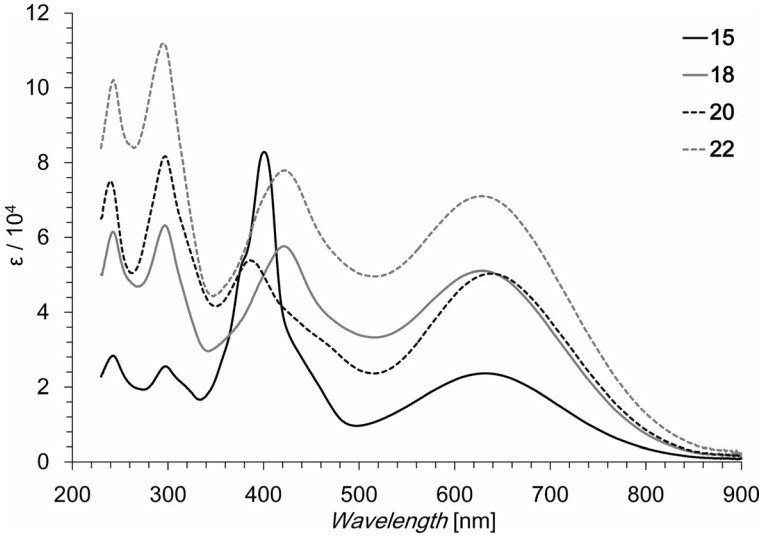

Figure 3. UV/visible spectra of DCNQ **15** (black line), **18** (gray line), **20** (broken black line) and **22** (broken gray line) in CH_2Cl_2.

Table 1. Absorption maxima [nm] and their coefficients (logε) of TCBDs and DCNQs **14**–**22** in CH_2Cl_2 and in hexane,[a–c] using TCBD **23**, DCNQ **24**, and **25** as references.

Sample	λ_{max} (logε) in CH_2Cl_2	λ_{max} (logε) in hexane
14	474 (4.49)	459 (4.49)[a]
15	631 (4.37)	593 (4.36)[b]
16	689 (4.52)	619 (4.48)[b]
17	489 (4.81)	459 (4.49)[a]
18	628 (4.71)	617 (4.71)[c]
19	456 (4.58)	449 (4.55)[a]
20	637 (4.70)	626 (4.69)[c]
21	503 (4.86)	488 (4.84)[a]
22	628 (4.85)	617 (4.83)[c]
23[8a]	462 (4.04)	–
24[8b]	641 (4.43)	598 (4.42)[b]
25[22]	676 (4.56)	600[b]

[a] CH_2Cl_2 was included in hexane to ensure solubility of the compounds. Measured in 20% CH_2Cl_2/hexane. [b] Measured in 10% CH_2Cl_2/hexane. [c] Measured in 50% CH_2Cl_2/hexane.

462 nm) (Figure 4), although the extinction coefficients still show the trend of increasing number of TCBD units. These effects are supported by the less effective π-conjugation between the central nitrogen atom and the TCBD units in **19**. Reduced π-conjugation in this system is possibly attributable to the diminished electron-donating potential of the carbazole spacer as rationalized by transient generation of a quinoidal structure supported by resonance structures.

DCNQ chromophores **15** and **16** exhibited a strong absorption band at λ_{max} = 631 nm and λ_{max} = 689 nm in CH_2Cl_2, respectively. Whereas the longest wavelength absorption maximum of **15** in the same spectral region resembles that of **24** at λ_{max} = 641 nm, the absorption maximum of **16** (λ_{max} = 689 nm) in CH_2Cl_2 was similar to that of simple DCNQ **25** (λ_{max} = 676 nm).[22] These results might be attributed to the effectiveness of ICT between the DCNQ unit and directly conjugated DMA groups, rather than the cross conjugated dicyanomethylidene unit. The absorption maxima of **18**, **20**, and **22** (**18**: 628 nm; **20**: 637 nm; **22**: 628 nm) were nearly identical to that observed for **15**, although the extinction coefficients were in proportion to the number of DCNQ units (Figure 4).

Most of the TCBD and DCNQ derivatives showed solvatochromism, when the solvent was changed from CH_2Cl_2 to hexane/CH_2Cl_2 mixtures. A noticeable spectral feature of **16** is the presence of a distinct absorption band at 689 nm in dichloromethane in which compound **16** exhibits blue-shifts of 70 nm (λ_{max} = 619 nm) in less polar 10% CH_2Cl_2/hexane, suggesting the ICT nature of this band (Figure 5).[23] The shift observed for DCNQs is larger than those of the corresponding TCNE adducts (TCBDs). This indicates that DCNQs possess higher polarity relative to the corresponding TCBDs with respect to UV/Vis spectral data.

To elucidate the nature of the absorption bands of **14**, **15**, and **16**, time-dependent density functional theory (TD-DFT) calculations at the B3LYP/6-31G(d) level were carried out on model compounds **14′**, **15′**, and **16′**, in which the isopropyl groups of **14**, **15**, and **16** were replaced with simple H atoms.[24] The frontier Kohn–Sham orbitals of these compounds are shown in the Supporting Information.

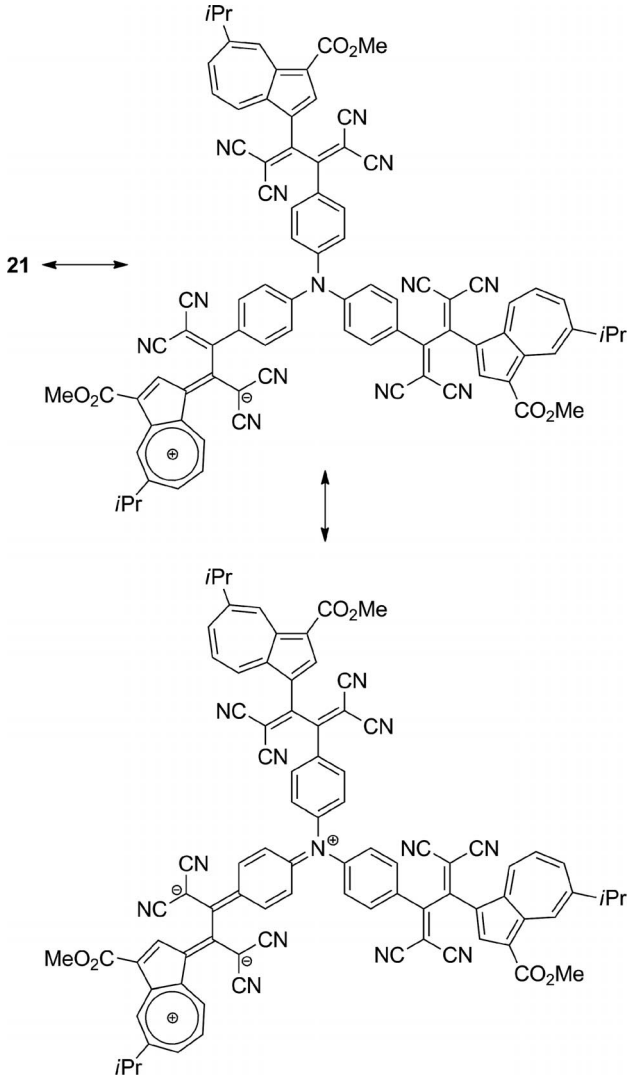

Scheme 9. Putative resonance structure of **21**.

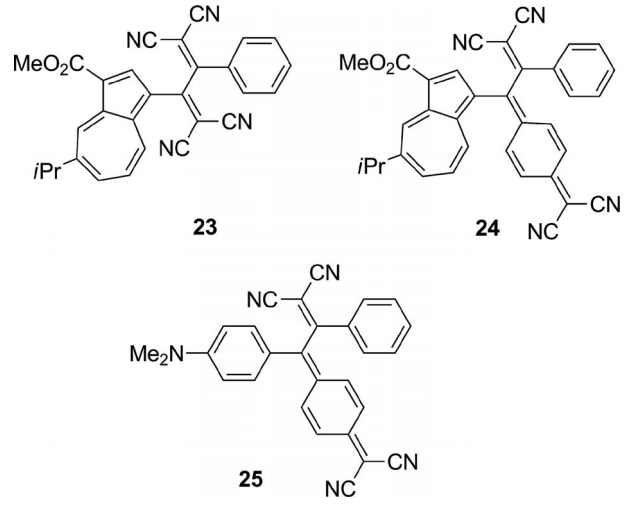

Figure 4. TCBD and DCNQ derivatives **23**–**25**.

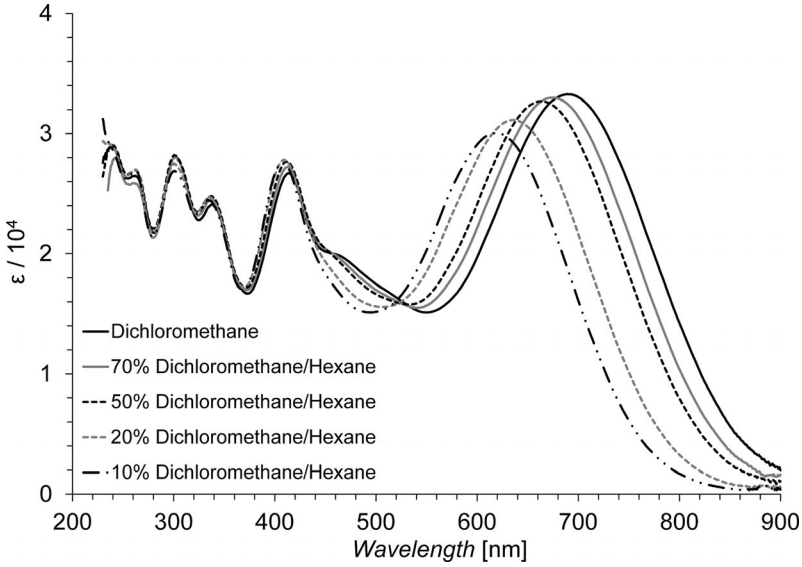

Figure 5. UV/Vis spectra of DCNQ **16** in CH_2Cl_2 and CH_2Cl_2/hexane (10%).

Based on comparisons of experimental and theoretical UV/Vis spectra, the absorption maxima of **14** in the visible region could be assigned to the transition originating from the HOMO located on DMA and the HOMO–1 located at the azulene ring to the LUMO located on the TCBD moiety. Thus, the broad absorption at λ_{max} = 474 nm for **14** could be attributed to overlapping of CT absorptions from the 1-azulenyl and DMA moieties to the TCBD unit.

Molecular orbital calculations performed on **15′** using B3LYP/6-31G(d) density functional theory revealed that the absorption band at λ_{max} = 595 nm of **15** is considered to overlap some transitions originating from the HOMO located on the 1-azulenyl group and HOMO–1 located on the DMA group to the LUMO and LUMO+2 located on the DCNQ moiety. The π–π* transitions of the substituted azulene moiety were confirmed from calculations of **15′** observed as the computed value at λ_{max} = 568 nm with relatively weak strength. ICT of **16′** was also confirmed by B3LYP/6-31G(d) density functional calculations; the longest absorption band was shown to arise due to overlapping of transitions shown in Table 2. The difference from the results using **15′** (relative to **16′**) was the effective contribution of HOMO→LUMO (i.e., transition between attached DMA and DCNQ moieties), compared with that from 1-azulenyl group to DCNQ. These results suggest that the longest wavelength absorption band has characteristics that are derived from the substituted aryl group conjugated directly with DCNQ moiety.

Table 2. Electronic transitions for **14′**, **15′**, and **16′** derived from computed values from **14**, **15**, and **16**.

Sample	Observed λ_{max} (log ε)	Computed λ_{max} (strength)	Composition of band[a]
14′	474 (4.49)[b]	493 (0.0738)	H→L (0.90)
		480 (0.0168)	H–1→L (0.32)
			H–1→L+1 (0.83)
			H→L+1 (0.37)
		457 (0.0712)	H–1→L (0.84)
			H–1→L+2 (0.39)
15′	593 (4.36)[c]	595 (0.0358)	H–1→L (0.97)
		568 (0.0070)	H→L+1 (0.97)
		515 (0.4537)	H→L (0.73)
			H→L+2 (0.52)
16′	619 (4.48)[c]	605 (0.3451)	H→L (0.78)
			H→L+2 (0.50)
		566 (0.0099)	H→L+1 (0.98)
		544 (0.1058)	H–2→L (0.23)
			H–1→L (0.91)

[a] H = HOMO; L = LUMO. [b] Measured in CH_2Cl_2. [c] Measured in 10% CH_2Cl_2/hexane.

Electrochemistry

To clarify their electrochemical properties, the redox behavior of **14**–**22** was examined by CV and DPV. Measurements were carried out with a standard three-electrode configuration. Tetraethylammonium perchlorate (0.1 M) in benzonitrile was used as a supporting electrolyte with platinum wire and disk as auxiliary and working electrodes, respectively. All measurements were carried out under an argon atmosphere, and potentials were related to an Ag/$AgNO_3$ reference electrode and Fc/Fc^+ as an internal reference, which discharges at +0.15 V under these conditions. A cyclic voltammogram for the reduction of **14** is shown in Figure 6. The redox potentials (in volts vs. Ag/$AgNO_3$) of **14**–**22** are summarized in Table 1.

The oxidation of these compounds was revealed in voltammograms that were characterized by irreversible oxidation waves, although a reversible oxidation wave was frequently observed in the arylamine derivatives. This is due to the generation of stabilized radical cationic species by electron removal from the nitrogen atom. The irreversible oxidation may be attributable to the destabilization of radical cationic species by the electron-withdrawing TCBD and DCNQ units.

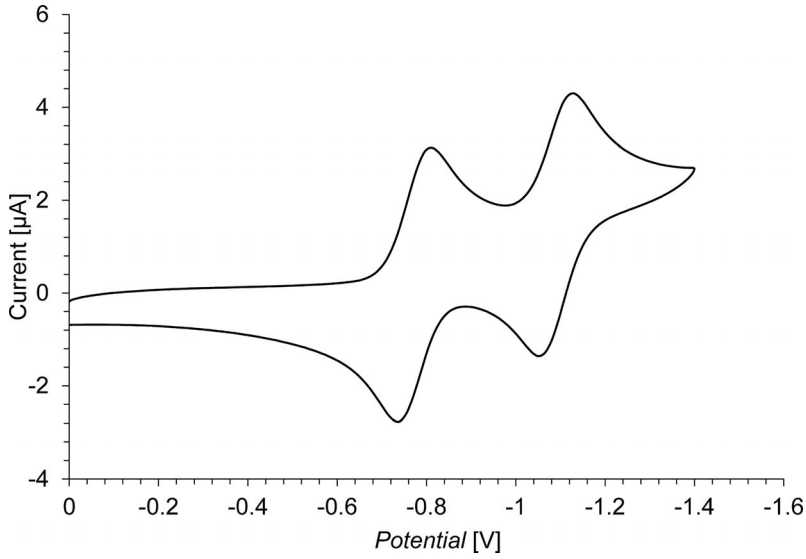

Figure 6. Cyclic voltammogram of **14** (1 mM) in benzonitrile containing Et_4NClO_4 (0.1 M) as a supporting electrolyte; scan rate = 100 mV s^{-1}.

Electrochemical reduction of TCBD derivatives **14**, **17**, **19**, and **21** displayed a reversible two- or three-stage wave, which contains multi-electron transfer in some cases. As shown in Table 3, the first reduction potentials of **14**, **17**, **19**, and **21** depend on the number of TCBD units in the molecule. Electrochemical reduction of **14** showed a reversible two-step reduction wave with half-wave potentials of –0.78 V and –1.09 V, which can probably be attributed to the formation of a stabilized radical anionic and a dianionic species, respectively (Figure 6).

A reversible three-stage wave was observed by CV in bis adducts **17** (–0.63 V, –0.72 V, and –1.06 V) and **19** (–0.64 V, –0.70 V, and –1.05 V), in which the third reduction waves were a two-electron transfer in one step to form a tetraanionic species. The electrochemical reduction of **21** also exhibited a reversible three-step reduction wave, whose potentials were identified at –0.58 V, –0.68 V, and –1.02 V by CV. The first reduction potentials of **14**, **17**, **19**, and **21** decreased in the order of number of TCBD units. This indicates that the connection of multiple TCBD units lowers the LUMO-level and increases the π-accepting property by effective π-conjugation with the arylamine cores.

Electrochemical reduction of DCNQs **15**, **16**, **18**, **20**, and **22** also showed a reversible two-stage reduction wave on CV, which could be attributed to the formation of radical anionic, dianionic species, and so on. The DCNQs **15**, **16**, **18**, **20**, and **22** exhibited more negative reduction potentials compared with those of the corresponding TCBD chromophores. These results are ascribed to the higher electron-accepting nature of the DCNQ moieties than that of the corresponding TCBD derivatives. The DMA-substituted TCBD **14** and DCNQ **15** showed more negative reduction potentials than those of corresponding **23** (E_1^{red} = –0.61 V) and **24** (E_1^{red} = –0.43 V). These results support the idea that the DMA moiety increases LUMO-levels due to its greater electron-donating character relative to that of the phenyl substituent.

Table 3. Redox potentials of TCBDs and DCNQs **14**–**22** bearing arylamine cores,[a,b] and TCBD **23** and DCNQ **24** as references.

Sample	Method	E_1^{red} [V]	E_2^{red} [V]	E_3^{red} [V]	E_4^{red} [V]
14	CV	–0.78	–1.09		
	(DPV)	(–0.76)	(–1.07)	(–1.98)	
15	CV	–0.54	–0.67		
	(DPV)	(–0.52)	(–0.65)	(–1.94)	
16	CV	–0.53	–0.67		
	(DPV)	(–0.51)	(–0.65)	(–1.87)	
17	CV	–0.63	–0.72	–1.06	
	(DPV)	(–0.61)	(–0.70)	(–1.04)	(–1.96)
18	CV	–0.51	–0.64		
	(DPV)	(–0.49)	(–0.62)	(–1.98)	
19	CV	–0.64	–0.70	–1.05	
	(DPV)	(–0.62)	(–0.68)	(–1.03)	(–1.96)
20	CV	–0.50	–0.64		
	(DPV)	(–0.48)	(–0.62)	(–2.00)	
21	CV	–0.58	–0.68	–1.02	
	(DPV)	(–0.56)	(–0.66)	(–1.00)	(–1.94)
22	CV	–0.46	–0.61		
	(DPV)	(–0.44)	(–0.59)	(–1.94)	
23	CV	–0.61	–1.03		
	(DPV)	(–0.59)	(–1.01)	(–1.95)	
24	CV	–0.43	–0.59		
	(DPV)	(–0.41)	(–0.57)	(–0.90)	(–1.93)

[a] V vs. $Ag/AgNO_3$, 1 mM in benzonitrile containing Et_4NClO_4 (0.1 M), Pt electrode (internal diameter: 1.6 mm), scan rate = 100 mV s^{-1}, and internal reference (Fc/Fc^+ = +0.15 V). [b] Half-wave potential $E^{red} = (E_{pc} + E_{pa})/2$ on CV, E_{pc} and E_{pa} correspond to the cathodic and anodic peak potentials, respectively.

We have reported the synthesis of various azulene-substituted redox-active chromophores with the aim of creating stabilized electrochromic materials.[25] In these studies, the TCBD units connected with π-electron systems exhibited stabilized electrochromism with strong absorptions in visible and near-infrared regions in their two-electron-reduced state. Thus, to examine color changes during the electrochemical reactions, spectral changes of the new TCBD and DCNQ derivatives were monitored by visible spectroscopy.

Constant-current reduction at room temperature was applied to solutions of chromophores **14**–**22**, with a platinum mesh as a working electrode and a wire counter-electrode, with visible spectra being measured in benzonitrile containing Et_4NClO_4 (0.1 M) as a supporting electrolyte (see the Supporting Information).

The longest absorption band noted for TCBD **14** at around 470 nm gradually decreased along with a development of the new absorption band at around 680 nm. The color of the solution gradually changed from red to yellow during electrochemical reduction. Reverse oxidation of the yellow-colored solution did not regenerate the spectrum of **14**, although good reversibility was observed in the two-step reduction on CV. The poor reversibility of the color changes might be attributable to the instability of the presumed dianionic species, due to destabilization by the electron-donating DMA unit. The longest absorption bands of the TCBD derivatives with arylamine cores **17**, **19**, and **21** also gradually decreased, and the color of the solution changed from red to yellow during electrochemical reduction. The reversible oxidation of the yellow solutions also did not regenerate the spectrum of the corresponding starting compounds (Figure 7).

When spectral changes of DCNQ **15** were monitored during electrochemical reduction, the absorption in the visible region gradually decreased with the development of new absorption bands at 755 nm and 860 nm, spreading over into the near-infrared region (Figure 8, top). The color change is attributable to the formation of anionic species formed by two-electron reduction of **15** (Figure 8, bottom). Reverse oxidation of the reduced species decreased the new absorption bands and regenerated the original color of **15**. The presumed redox behavior of **15** is illustrated in Scheme 10. As suggested by the CV results, the color change noted for **15** should be ascribed by the two electron reduction of the DCNQ unit to form dianionic species,

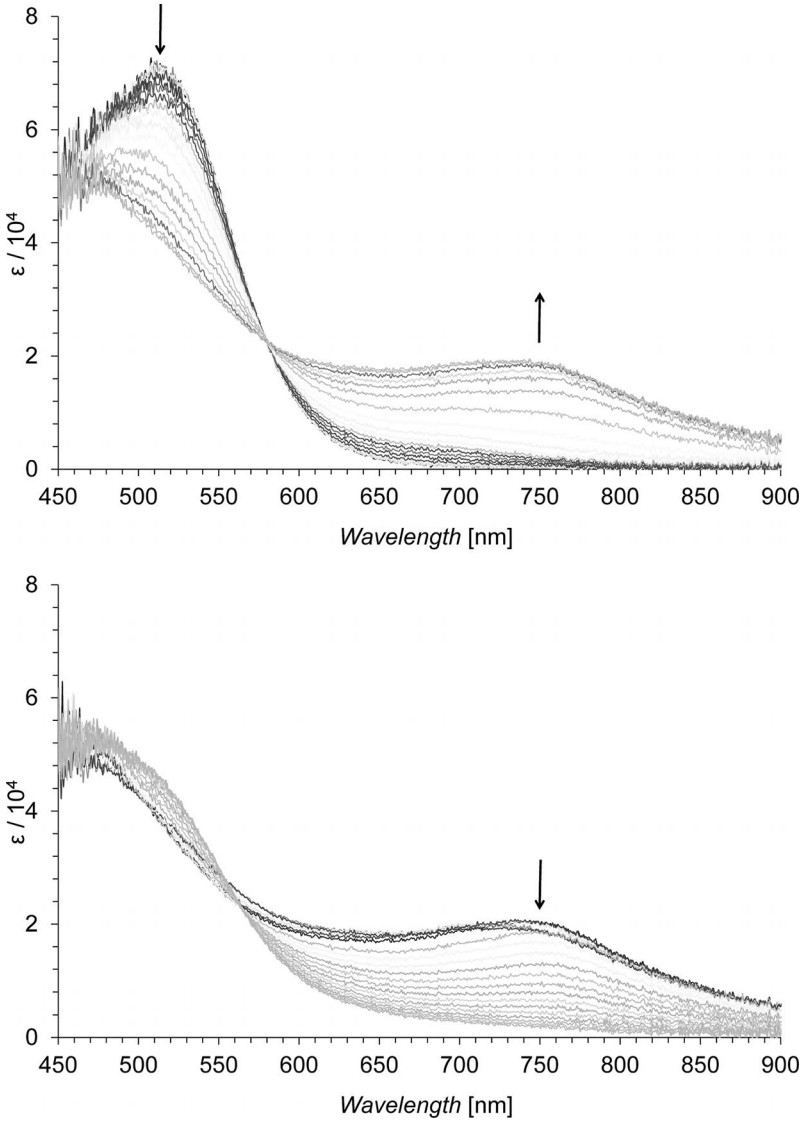

Figure 7. Continuous change in the UV/Vis spectrum of **17**: constant-current electrochemical reduction (100 μA, top) and reverse oxidation of the reduced species (100 μA, bottom) in benzonitrile containing Et_4NClO_4 (0.1 M) at 30 sec intervals.

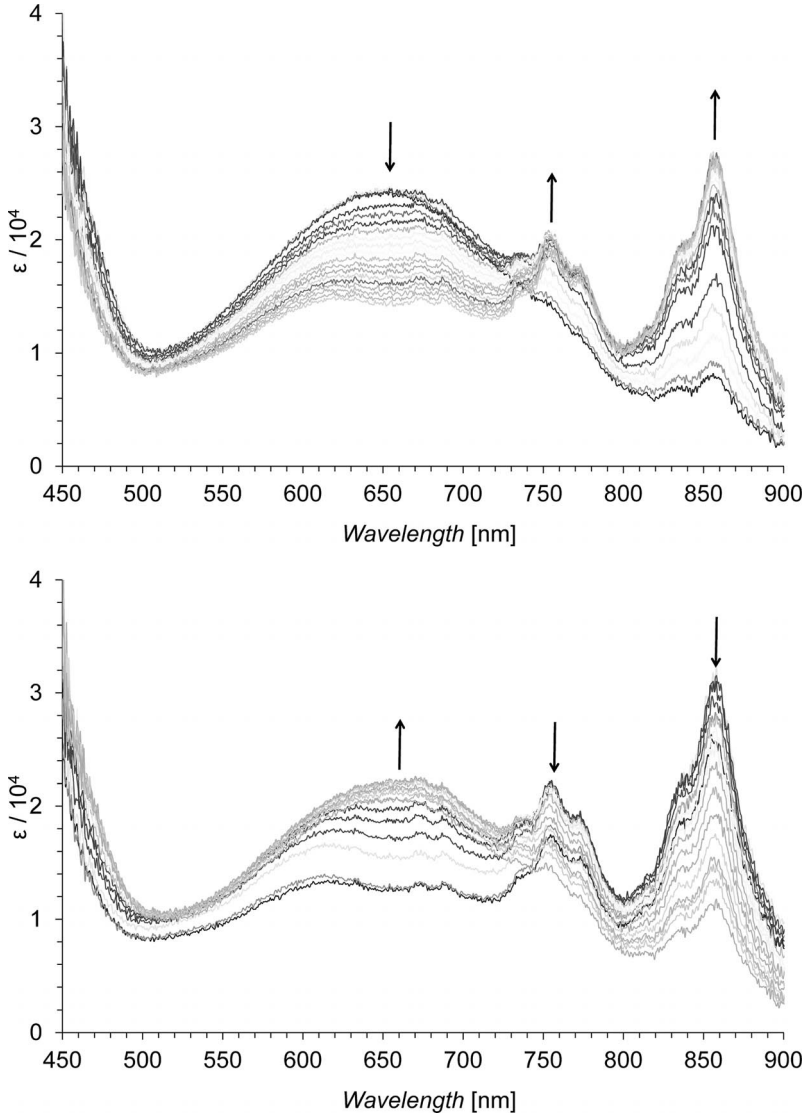

Figure 8. Continuous change in the UV/Vis spectrum of **15**: constant-current electrochemical reduction (100 μA, top) and reverse oxidation of the reduced species (100 μA, bottom) in benzonitrile containing Et_4NClO_4 (0.1 M) at 30 sec intervals.

which could be described as a closed-shell form as illustrated in Scheme 10. The longest absorption band of DCNQ **16** gradually decreased, and the color of the solution changed from dark-green to yellow during the electrochemical reduction. Reversible oxidation of the yellow-colored solution partially regenerated the spectra of the corresponding original compound. The absorption bands of **17** in the visible region disappeared along with an increase in the new absorption maxima around 750 nm during the electrochemical reduction. The color of the solution gradually changed from red to yellow during the electrochemical reduction. The reverse oxidation of the transient yellow solution did not regenerate the parent spectrum of **17**. When visible spectra of **18** were measured under electrochemical reduction conditions, absorption of **18** in the visible region gradually decreased coincident with a color change from green to yellow. However, reverse oxidation did not regenerate the original absorption of **18**. When the visible spectra

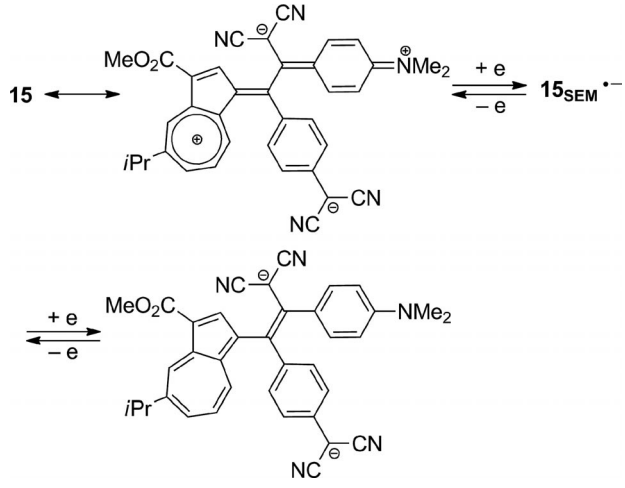

Scheme 10. Presumed redox behavior of DCNQ **15** (SEM is the semiquinone state formed by the single-electron transfer).

of **20** were measured under electrochemical reduction conditions, the absorption band for **20** in the visible region at around 650 nm gradually decreased. Reverse oxidation of the reduced species diminished the new absorption bands, but did not completely regenerate the absorption band of **20**. The greenish-blue color of the solution for **22** changed to yellow during electrochemical reduction, and reverse oxidation of the yellow-colored solution regenerated the visible spectra of **22**.

Conclusions

Arylamine derivatives with pendant 1-azulenylethynyl groups **10**–**14** were prepared by Sonogashira–Hagihara cross-coupling chemistry. A series of TCBD and DCNQ chromophores substituted by the 1-azulenyl groups were synthesized in a one-pot reaction consisting of the formal [2+2] cycloaddition reaction of **10**–**14** with TCNE and TCNQ, followed by ring-opening reaction of the initially formed cyclobutene derivatives. Strong intramolecular CT absorption bands were observed in the UV/Vis spectra of these azulene-substituted TCBD and DCNQ derivatives. An analysis by CV and DPV revealed that chromophores **14**–**21** exhibit reversible two- or three stage reduction waves. Moreover, a significant color change was observed during the electrochemical reduction. In particular, DCNQ **15** exhibited a significant color change, arising from the generation of a stable dianionic structure during electrochemical reduction.

Experimental Section

General: Melting points were determined with a Yanagimoto MPS3 micro melting apparatus and are uncorrected. Mass spectra were obtained with Bruker APEX II instruments. IR and UV/Vis spectra were measured with JASCO FT/IR-4100 and Shimadzu UV-2550 spectrophotometers, respectively. ^{1}H and ^{13}C NMR spectra were recorded with a JEOL ECA-500 spectrometer (at 500 MHz and 125 MHz, respectively). Voltammetry measurements were carried out using a BAS 100B/W electrochemical workstation equipped with Pt working and auxiliary electrodes and a reference electrode formed from $Ag/AgNO_3$ (0.01 M) in acetonitrile containing tetrabutylammonium perchlorate (0.1 M). Elemental analyses were performed at the Research and Analytical Center for Giant Molecules, Graduate School of Science, Tohoku University.

Compound 10: To a solution of **9** (252 mg, 1.00 mmol), **5** (272 mg, 1.10 mmol), and CuI (19 mg, 0.10 mmol) in triethylamine (10 mL) and THF (10 mL) was added tetrakis(triphenylphosphine)palladium(0) (58 mg, 0.05 mmol). The resulting mixture was stirred at room temperature for 1 h under an Ar atmosphere. The reaction mixture was poured into a 10% NH_4Cl solution and extracted with CH_2Cl_2. The organic layer was washed with brine, dried with Na_2SO_4, and concentrated under reduced pressure. The residue was purified by column chromatography on silica gel with CH_2Cl_2 to give **10** (368 mg, 99%) as green crystals, m.p. 154.0–158.0 °C (CH_2Cl_2). IR (KBr disk): $\tilde{\nu}_{max}$ = 2961 (w), 2197 (w), 1692 (m), 1602 (m), 1527 (m), 1444 (s), 1367 (m), 1235 (s), 1203 (s), 1122 (w), 1071 (w), 1040 (w), 951 (w), 881 (w), 809 (m), 783 (w) cm^{-1}. UV/Vis (CH_2Cl_2): λ_{max} (log ε) = 248 (4.36), 300 (4.64), 332 sh (4.54), 409 (4.06), 440 sh (3.91), 589 (2.81) nm. ^{1}H NMR (500 MHz, $CDCl_3$): δ_H = 9.68 (d, *J* = 2.0 Hz, 1 H, 4-H), 8.64 (d, *J* = 10.0 Hz, 1 H, 8-H), 8.42 (s, 1 H, 2-H), 7.76 (d, *J* = 10.0 Hz, 1 H, 6-H), 7.47 (d, *J* = 9.0 Hz, 2 H, 2′,6′-H), 7.45 (t, *J* = 10.0 Hz, 1 H, 7-H), 6.69 (d, *J* = 9.0 Hz, 2 H, 3′,5′-H), 3.95 (s, 3 H, CO_2Me), 3.21 (sept, *J* = 6.5 Hz, 2 H, *i*Pr), 3.00 (s, 6 H, NMe_2), 1.42 (d, *J* = 6.5 Hz, 6 H, *i*Pr) ppm. ^{13}C NMR (125 MHz, $CDCl_3$): δ_C = 165.68 (CO_2Me), 150.08 (C-1′), 150.01 (C-5), 144.54 (C-3a), 142.44 (C-2), 141.13 (C-8a), 139.16 (C-6), 138.11 (C-4), 136.39 (C-8), 132.61 (C-2′,6′), 127.13 (C-7), 114.88 (C-3), 112.05 (C-3′,5′), 110.82 (C-4′), 110.31 (C-1), 94.69 (C≡C), 82.44 (C≡C), 51.24 (CO_2Me), 40.40 (NMe_2), 39.33 (*i*Pr), 24.73 (*i*Pr) ppm. HRMS (FAB) calcd. for $C_{25}H_{25}NO_2$ $[M]^+$ 371.1880, found 371.1885; $C_{25}H_{25}NO_2$ (371.47): C, 80.83; H, 6.78; N, 3.77; found C, 80.69; H, 6.79; N 3.61.

Compound 11: To a solution of **9** (555 mg, 2.20 mmol), **6** (421 mg, 1.00 mmol), and CuI (38 mg, 0.20 mmol) in triethylamine (15 mL) and THF (15 mL) was added tetrakis(triphenylphosphine)palladium(0) (116 mg, 0.10 mmol). The resulting mixture was stirred at 50 °C for 3 h under an Ar atmosphere. The reaction mixture was poured into a 10% NH_4Cl solution and extracted with CH_2Cl_2. The organic layer was washed with brine, dried with Na_2SO_4, and concentrated under reduced pressure. The residue was purified by column chromatography on silica gel with CH_2Cl_2 to give **11** (630 mg, 94%) as green crystals, m.p. 110.0–114.0 °C (CH_2Cl_2). IR (KBr disk): $\tilde{\nu}_{max}$ = 3348 (w), 2957 (w), 2196 (w), 1687 (s), 1597 (m), 1508 (s), 1447 (s), 1321 (m), 1241 (m), 1206 (s), 1124 (w), 1043 (w), 961 (w), 925 (w), 877 (w), 818 (m), 765 (m) cm^{-1}. UV/Vis (CH_2Cl_2): λ_{max} (log ε) = 246 (4.69), 276 sh (4.57), 302 (4.76), 312 sh (4.75), 358 (4.76), 407 (4.54), 434 sh (4.42), 580 (3.11) nm. ^{1}H NMR (500 MHz, $CDCl_3$): δ_H = 9.72 (d, *J* = 1.5 Hz, 2 H, 4-H), 8.65 (d, *J* = 10.0 Hz, 2 H, 8-H), 8.46 (s, 2 H, 2-H), 7.79 (d, *J* = 10.0 Hz, 2 H, 6-H), 7.53 (d, *J* = 8.5 Hz, 4 H, 2′,2′′,6′,6′′-H), 7.49 (t, *J* = 10.0 Hz, 2 H, 7-H), 7.10 (d, *J* = 8.5 Hz, 2 H, 3′,3′′,5′,5′′-H), 5.99 (s, 1 H, NH), 3.96 (s, 6 H, CO_2Me), 3.22 (sept, *J* = 6.5 Hz, 2 H, *i*Pr), 1.42 (d, *J* = 6.5 Hz, 12 H, *i*Pr) ppm. ^{13}C NMR (125 MHz, $CDCl_3$): δ_C = 165.52 (CO_2Me), 150.34 (C-5), 144.63 (C-3a or 8a), 142.53 (C-2), 142.01 (C-3a or 8a), 141.15 (C-1′,1′′), 139.23 (C-6), 138.19 (C-4), 136.23 (C-8), 132.68 (C-2′,2′′,6′,6′′), 127.27 (C-5), 117.54 (C-3′,3′′,5′,5′′), 116.27 (C-4′,4′′), 114.94 (C-3), 109.52 (C-1), 93.76 (C≡C), 83.64 (C≡C), 51.15 (CO_2Me), 39.20 (*i*Pr), 24.58 (*i*Pr) ppm. HRMS (FAB) calcd. for $C_{46}H_{39}NO_4^+$ $[M]^+$ 669.2874, found 669.2872. $C_{46}H_{39}NO_4 \cdot 1/2H_2O$ (669.81): calcd. C 81.39, H 5.94, N 2.06; found C 81.41, H 5.94, N 2.05.

Compound 12: To a solution of **9** (555 mg, 2.20 mmol), **7** (419 mg, 1.00 mmol), and CuI (38 mg, 0.20 mmol) in triethylamine (15 mL) and THF (15 mL) was added tetrakis(triphenylphosphine)palladium(0) (116 mg, 0.10 mmol). The resulting mixture was stirred at 50 °C for 5 h under an Ar atmosphere. The reaction mixture was poured into a 10% NH_4Cl solution and extracted with CH_2Cl_2. The organic layer was washed with brine, dried with Na_2SO_4, and concentrated under reduced pressure. The residue was purified by column chromatography on silica gel with CH_2Cl_2 to give **12** (568 mg, 85%) as green crystals, m.p. 135.0–139.0 °C (CH_2Cl_2). IR (KBr disk): $\tilde{\nu}_{max}$ = 3348 (w), 2956 (w), 2874 (w), 2196 (w), 1686 (s), 1603 (w), 1477 (s), 1446 (s), 1278 (w), 1245 (m), 1214 (s), 1169 (m), 1125 (m), 1043 (w), 877 (w), 807 (m), 767 (m) cm^{-1}. UV/Vis (CH_2Cl_2): λ_{max} (log ε) = 249 (4.84), 282 sh (4.79), 305 sh (4.89), 316 (4.90), 406 (4.42), 425 sh (4.33), 581 (3.11) nm. ^{1}H NMR (500 MHz, $CDCl_3$): δ_H = 9.72 (d, *J* = 2.0 Hz, 2 H, 4-H), 8.73 (d, *J* = 10.0 Hz, 2 H, 8-H), 8.50 (s, 2 H, 2-H), 8.35 (s, 2 H, 4′,5′-H), 8.32 (s, 1 H, NH), 7.80 (d, *J* = 10.0 Hz, 2 H, 6-H), 7.68 (d, *J* = 8.5 Hz, 2 H, 2′,7′-H), 7.52 (t, *J* = 10.0 Hz, 2 H, 7-H), 7.42 (d, *J* = 8.5 Hz, 2 H, 1′,8′-H), 3.97 (s, 6 H, CO_2Me), 3.23 (sept, *J* = 6.5 Hz, 2 H,

*i*Pr), 1.43 (d, *J* = 6.5 Hz, 12 H, *i*Pr) ppm. ^{13}C NMR (125 MHz, $CDCl_3$): δ_C = 165.59 (CO_2Me), 150.32 (C-5), 144.71 (C-3a), 142.56 (C-2), 141.17 (C-8a), 139.24 (C-6), 138.19 (C-4), 136.31 (C-8), 129.80 (C-2′,7′), 127.30 (C-7), 123.84 (C-2), 123.10 (C-4a′,4b′), 115.20 (C-8a′,9a′), 114.93 (C-3), 110.90 (C-1′,8′), 109.68 (C-1), 94.58 (C≡C), 83.04 (C≡C), 51.17 (CO_2Me), 39.22 (*i*Pr), 24.60 (*i*Pr) ppm. HRMS (FAB) calcd. for $C_{46}H_{37}NO_4^+$ $[M]^+$ 667.2718, found 667.2703. $C_{46}H_{37}NO_4 \cdot 1/2H_2O$ (667.79): calcd. C 81.63, H 5.66, N 2.07; found C 81.60, H 5.64, N 2.05.

Compound 13: To a solution of **9** (833 mg, 3.30 mmol), **8** (623 mg, 1.00 mmol), and CuI (57 mg, 0.30 mmol) in triethylamine (15 mL) and THF (15 mL) was added tetrakis(triphenylphosphine)palladium(0) (173 mg, 0.15 mmol). The resulting mixture was stirred at 50 °C for 6 h under an Ar atmosphere. The reaction mixture was poured into a 10% NH_4Cl solution and extracted with CH_2Cl_2. The organic layer was washed with brine, dried with Na_2SO_4, and concentrated under reduced pressure. The residue was purified by column chromatography on silica gel with CH_2Cl_2 to give **13** (897 mg, 90%) as green crystals, m.p. 131.0–133.0 °C ($CHCl_3$/MeOH). IR (KBr disk): $\tilde{\nu}_{max}$ = 2957 (w), 2196 (w), 1693 (s), 1593 (w), 1496 (s), 1446 (s), 1381 (w), 1317 (m), 1280 (m), 1245 (m), 1204 (s), 1123 (m), 1044 (w), 958 (w), 919 (w), 877 (w), 831 (m), 776 (m), 726 (w) cm^{-1}. UV/Vis (CH_2Cl_2): λ_{max} (log ε) = 247 (4.88), 306 (4.93), 370 (4.86), 408 (4.77), 433 sh (4.68), 576 (3.32) nm. ^{1}H NMR (500 MHz, $CDCl_3$): δ_H = 9.72 (d, *J* = 1.5 Hz, 3 H, 4-H), 8.65 (d, *J* = 10.0 Hz, 3 H, 8-H), 8.46 (s, 3 H, 2-H), 7.80 (d, *J* = 10.0 Hz, 3 H, 6-H), 7.52 (d, *J* = 8.5 Hz, 6 H, 3′,5′-H), 7.50 (dd, *J* = 10.0, 10.0 Hz, 3 H, 7-H), 7.14 (d, *J* = 8.5 Hz, 6 H, 2′,6′-H), 3.96 (s, 9 H, CO_2Me), 3.24 (sept, *J* = 7.0 Hz, 3 H, *i*Pr), 1.48 (d, *J* = 7.0 Hz, 18 H, *i*Pr) ppm. ^{13}C NMR (125 MHz, $CDCl_3$): δ_C = 165.45 (CO_2Me), 150.47 (C-5), 146.38 (C-1′), 144.69 (C-3a), 142.60 (C-2), 141.19 (C-8a), 139.28 (C-6), 138.25 (C-4), 136.20 (C-8), 132.51 (C-3′,5′), 127.37 (C-7), 124.07 (C-2′,6′), 118.51 (C-4′), 114.99 (C-3), 109.24 (C-1), 93.49 (C≡C), 84.63 (C≡C), 51.18 (CO_2Me), 39.24 (*i*Pr), 24.61 (*i*Pr) ppm. HRMS (FAB) calcd. for $C_{69}H_{57}NO_6^+$ $[M]^+$ 995.4181, found 995.4185. $C_{69}H_{57}NO_6 \cdot 1/10CHCl_3$ (996.19): calcd. C 82.32, H 5.71, N 1.39; found C 82.27, H 5.81, N 1.41.

Compound 14: To a solution of **10** (186 mg, 0.50 mmol) in EtOAc (5 mL) was added TCNE (77 mg, 0.60 mmol). The resulting mixture was refluxed for 1 h under an Ar atmosphere. The solvent was removed under reduced pressure. The residue was purified by column chromatography on silica gel with CH_2Cl_2/EtOAc (20:1) to give **14** (242 mg, 97%) as red crystals, m.p. 159.0–162.0 °C (CH_2Cl_2/hexane). IR (KBr disk): $\tilde{\nu}_{max}$ = 2955 (w), 2213 (m), 1701 (m), 1603 (s), 1488 (s), 1438 (s), 1418 (m), 1383 (m), 1336 (m), 1295 (w), 1241 (w), 1210 (s), 1174 (s), 1055 (w), 943 (w), 902 (w), 814 (w), 779 (w), 735 (w) cm^{-1}. UV/Vis (CH_2Cl_2): λ_{max} (log ε) = 250 (4.44), 265 sh (4.42), 303 (4.65), 346 sh (4.17), 391 sh (4.24), 474 (4.49) nm. UV/Vis (20% CH_2Cl_2/hexane): λ_{max} (log ε) = 246 (4.44), 265 sh (4.43), 300 (4.38), 346 sh (4.19), 389 (4.25), 459 (4.49) nm. ^{1}H NMR (500 MHz, $CDCl_3$): δ_H = 9.97 (d, *J* = 2.0 Hz, 1 H, 4-H), 8.51 (d, *J* = 10.0 Hz, 1 H, 8-H), 8.31 (s, 1 H, 2-H), 8.11 (d, *J* = 10.0 Hz, 1 H, 6-H), 7.93 (dd, *J* = 10.0, 10.0 Hz, 1 H, 7-H), 7.92 (d, *J* = 9.0 Hz, 2 H, 2′,6′-H), 6.78 (d, *J* = 9.0 Hz, 2 H, 3′,5′-H), 3.93 (s, 3 H, CO_2Me), 3.34 (sept, *J* = 7.0 Hz, 1 H, *i*Pr), 3.19 (s, 6 H, NMe_2), 1.47 (d, *J* = 7.0 Hz, 6 H, *i*Pr) ppm. ^{13}C NMR (125 MHz, $CDCl_3$): δ_C = 165.54 (CO_2Me), 164.57 [*C*=C(CN)$_2$], 162.92 [*C*=C(CN)$_2$], 156.34 (C-5), 154.36 (C-1′), 145.98 (C-8a), 142.93 (C-2), 142.09 (C-6), 141.87 (C-3a), 140.36 (C-4), 137.71 (C-8), 132.82 (C-2′,6′), 131.95 (C-7), 120.07 (C-1), 119.18 (C-3), 118.94 (C-4′), 114.64 (CN), 114.07 (CN), 113.53 (CN), 112.66 (CN), 112.24 (C-3′,5′), 80.54 [*C*(CN)$_2$], 74.85 [*C*(CN)$_2$], 51.59 (CO_2Me), 40.18 (NMe_2), 39.43 (*i*Pr), 24.49 (*i*Pr) ppm. HRMS (FAB) calcd. for $C_{31}H_{25}N_5O_2^+$ $[M]^+$ 499.2003, found 499.2006. $C_{31}H_{25}N_5O_2$ (499.56): calcd. C 74.53, H 5.04, N 14.02; found C 74.39, H 4.88, N 13.98.

Reaction of 10 with TCNQ: To a solution of **10** (186 mg, 0.50 mmol) in EtOAc (10 mL) was added TCNQ (123 mg, 0.60 mmol). The resulting mixture was refluxed for 12 h under an Ar atmosphere. The solvent was removed under reduced pressure. The residue was purified by column chromatography on silica gel with CH_2Cl_2/EtOAc (10:1) to give **15** (124 mg, 43%) as dark green crystals and **16** (138 mg, 48%) as dark green crystals, respectively.

Compound 15: M.p. 181.0–184.0 °C (CH_2Cl_2/hexane). IR (KBr disk): $\tilde{\nu}_{max}$ = 2960 (w), 2927 (w), 2207 (m), 1698 (m), 1602 (s), 1540 (w), 1490 (m), 1438 (s), 1420 (m), 1379 (s), 1330 (m), 1288 (w), 1210 (s), 1189 (s), 1172 (s), 1130 (w), 1087 (w), 1046 (w), 998 (w), 972 (w), 943 (w), 903 (w), 860 (w), 838 (w), 820 (w), 780 (w), 700 (w), 670 (w) cm^{-1}. UV/Vis (CH_2Cl_2): λ_{max} (log ε) = 243 (4.45), 298 (4.41), 377 sh (4.72), 401 (4.92), 453 sh (4.35), 631 (4.37) nm. UV/Vis (10% CH_2Cl_2/hexane): λ_{max} (log ε) = 242 (4.45), 297 (4.41), 374 (4.75), 393 (4.97), 593 (4.36) nm. ^{1}H NMR (500 MHz, $CDCl_3$): δ_H = 9.88 (d, *J* = 1.5 Hz, 1 H, 4-H), 8.38 (d, *J* = 10.0 Hz, 1 H, 8-H), 8.18 (s, 1 H, 2-H), 7.97 (d, *J* = 10.0 Hz, 1 H, 6-H), 7.79 (d, *J* = 9.5 Hz, 2 H, 2′,6′-H), 7.65 (dd, *J* = 10.0, 10.0 Hz, 1 H, 7-H), 7.15–7.05 (m, 4 H, H_{DCNQ}), 6.67 (d, *J* = 9.5 Hz, 2 H, 3′,5′-H), 3.94 (s, 3 H, CO_2Me), 3.30 (sept, *J* = 7.0 Hz, 1 H, *i*Pr), 3.13 (s, 6 H, NMe_2), 1.45 (d, *J* = 7.0 Hz, 6 H, *i*Pr) ppm. ^{13}C NMR (125 MHz, $CDCl_3$): δ_C = 169.29 (C_{DCNQ}), 164.79 (CO_2Me), 154.58 (C-5), 154.27 [*C*=C(CN)$_2$], 153.87 [*C*=C(CN)$_2$], 148.25 (C-1′), 144.96 (C-8a), 143.73 (C-3a), 143.67 (C-2), 141.43 (C-6), 139.99 (C-4), 136.69 (C-8), 136.29 (C_{DCNQ}), 134.55 (C_{DCNQ}), 132.79 (C-2′,6′), 132.57, 130.94 (C-7), 125.09 (C_{DCNQ}), 124.95 (C-1), 124.60 (C_{DCNQ}), 121.54 (C-4′), 118.79 (C-3), 115.26 (CN), 114.48 (CN), 114.39 (CN), 114.26 (CN), 111.93 (C-3′,5′), 76.38 [*C*(CN)$_2$], 73.01 [*C*(CN)$_2$], 51.51 (CO_2Me), 40.10 (NMe_2), 39.34 (*i*Pr), 24.49 (*i*Pr) ppm. HRMS (FAB) calcd. for $C_{37}H_{29}N_5O_2^+$ $[M]^+$ 575.2316, found 575.2340. $C_{37}H_{29}N_5O_2$ (575.66): calcd. C 77.20, H 5.08, N 12.17; found C 77.08, H 5.19, N 12.13.

Compound 16: M.p. 183.0–187.0 °C decomp. (CH_2Cl_2/hexane). IR (KBr disk): $\tilde{\nu}_{max}$ = 2956 (w), 2202 (m), 1697 (m), 1581 (s), 1485 (w), 1440 (m), 1417 (m), 1367 (s), 1347 (s), 1325 (w), 1273 (w), 1231 (w), 1221 (w), 1169 (s), 1130 (w), 1048 (w), 998 (w), 942 (w), 908 (w), 838 (w), 818 (w), 793 (w), 746 (w), 725 (w), 674 (w) cm^{-1}. UV/Vis (CH_2Cl_2): λ_{max} (log ε) = 238 (4.46), 262 (4.42), 301 (4.45), 338 (4.38), 415 (4.43), 462 sh (4.30), 689 (4.52) nm. UV/Vis (10% CH_2Cl_2/hexane): λ_{max} (log ε) = 262 (4.43), 301 (4.43), 334 (4.39), 409 (4.44), 619 (4.48) nm. ^{1}H NMR (500 MHz, $CDCl_3$): δ_H = 9.93 (d, *J* = 1.5 Hz, 1 H, 4-H), 8.57 (s, 1 H, 2-H), 8.45 (d, *J* = 10.0 Hz, 1 H, 8-H), 8.02 (d, *J* = 10.0 Hz, 1 H, 6-H), 7.76 (dd, *J* = 10.0, 10.0 Hz, 1 H, 7-H), 7.51 (dd, *J* = 9.5, 2.0 Hz, 1 H, H_{DCNQ}), 7.36 (d, *J* = 9.0 Hz, 2 H, 2′,6′-H), 7.24 (dd, *J* = 9.5, 2.0 Hz, 1 H, H_{DCNQ}), 7.02 (dd, *J* = 9.5, 2.0 Hz, 1 H, H_{DCNQ}), 6.98 (dd, *J* = 9.5, 2.0 Hz, 1 H, H_{DCNQ}), 6.70 (d, *J* = 9.0 Hz, 2 H, 3′,5′-H), 3.93 (s, 3 H, CO_2Me), 3.30 (sept, *J* = 7.0 Hz, 1 H, *i*Pr), 3.12 (s, 6 H, NMe_2), 1.44 (d, *J* = 7.0 Hz, 6 H, *i*Pr) ppm. ^{13}C NMR (125 MHz, $CDCl_3$): δ_C = 166.28, 164.63 (CO_2Me), 155.62, 154.09, 153.97, 152.86, 145.55, 143.25, 141.67, 141.57, 140.20, 136.43, 136.07, 134.99, 134.45, 132.78, 132.62, 131.22, 125.14, 125.02, 124.49, 122.84, 118.47, 114.95, 114.82 (CN), 113.53 (CN), 112.47 (CN), 111.91 (CN), 82.35 [*C*(CN)$_2$], 70.89 [*C*(CN)$_2$], 51.62 (CO_2Me), 40.18 (NMe_2), 39.33 (*i*Pr), 24.46 (*i*Pr) ppm. HRMS (FAB) calcd. for $C_{37}H_{29}N_5O_2^+$ $[M]^+$ 575.2316, found 575.2313. $C_{37}H_{29}N_5O_2$ (575.66): calcd. C 77.20, H 5.08, N 12.17; found C 77.11, H 5.16, N 12.15.

Compound 17: To a solution of **11** (201 mg, 0.30 mmol) in EtOAc (10 mL) was added TCNE (102 mg, 0.80 mmol). The resulting mixture was refluxed for 6 h under an Ar atmosphere. The solvent was removed under reduced pressure. The residue was purified by column chromatography on silica gel with CH_2Cl_2/EtOAc (20:1) to give **17** (272 mg, 98%) as red crystals, m.p. 170.0–172.0 °C (CH_2Cl_2/hexane). IR (KBr disk): $\tilde{\nu}_{max}$ = 2953 (w), 2224 (m), 1700 (m), 1588 (s), 1489 (s), 1439 (m), 1418 (m), 1383 (m), 1284 (w), 1240 (w), 1212 (w), 1179 (s), 1093 (w), 1041 (w), 902 (w), 817 (w), 777 (w), 729 (w), 664 (w) cm^{-1}. UV/Vis (CH_2Cl_2): λ_{max} (log ε) = 262 (4.80), 300 (4.74), 340 sh (4.57), 389 sh (4.48), 489 (4.81) nm. UV/Vis (20% CH_2Cl_2/hexane): λ_{max} (log ε) = 246 (4.44), 262 (4.43), 300 (4.38), 341 sh (4.21), 389 (4.25), 459 (4.49) nm. ^{1}H NMR (500 MHz, $CDCl_3$): δ_H = 10.00 (d, *J* = 2.0 Hz, 2 H, 4-H), 8.49 (d, *J* = 10.0 Hz, 2 H, 8-H), 8.30 (s, 2 H, 2-H), 8.16 (d, *J* = 10.0 Hz, 2 H, 6-H), 7.99 (d, *J* = 10.0 Hz, 2 H, 7-H), 7.90 (d, *J* = 8.5 Hz, 4 H, 2′,6′-H), 7.32 (d, *J* = 8.5 Hz, 4 H, 3′,5′-H), 7.29 (s, 1 H, NH), 3.95 (s, 6 H, CO_2Me), 3.35 (sept, *J* = 7.0 Hz, 2 H, *i*Pr), 1.47 (d, *J* = 7.0 Hz, 12 H, *i*Pr) ppm. ^{13}C NMR (125 MHz, $CDCl_3$): δ_C = 167.05 (C-1′), 164.41 (CO_2Me), 161.16 [*C*=C(CN)$_2$], 157.13 (C-5), 146.25 [*C*=C(CN)$_2$], 146.21 (C-8a), 142.61 (C-2 or 6), 142.58 (C-2 or 6), 142.00 (C-3a), 140.77 (C-4), 137.68 (C-8), 132.44 (C-2′,6′), 132.38 (C-7), 125.86 (C-4′), 119.69 (C-1), 119.51 (C-3), 118.52 (C-3′,5′), 113.75 (CN), 112.96 (CN), 112.66 (CN), 111.86 (CN), 83.19 [*C*(CN)$_2$], 80.33 [*C*(CN)$_2$], 51.76 (CO_2Me), 39.51 (*i*Pr), 24.49 (*i*Pr) ppm. HRMS (FAB) calcd. for $C_{58}H_{39}N_9O_4^+$ $[M]^+$ 925.3120, found 925.3139. $C_{58}H_{39}N_9O_4$ (925.99): calcd. C 75.23, H 4.25, N 13.61; found C 75.10, H 4.38, N 13.57.

Compound 18: To a solution of **11** (201 mg, 0.30 mmol) in EtOAc (15 mL) was added TCNQ (204 mg, 1.00 mmol). The resulting mixture was refluxed for 12 h under an Ar atmosphere. The solvent was removed under reduced pressure. The residue was purified by column chromatography on silica gel with CH_2Cl_2/EtOAc (10:1) to give **18** (294 mg, 91%) as dark green crystals, m.p. 246.0–248.0 °C (CH_2Cl_2/hexane). IR (KBr disk): $\tilde{\nu}_{max}$ = 2961 (w), 2208 (m), 1698 (m), 1588 (s), 1505 (s), 1439 (s), 1420 (m), 1398 (m), 1381 (m), 1350 (m), 1317 (m), 1279 (m), 1214 (s), 1189 (s), 1128 (w), 1085 (w), 1046 (w), 974 (w), 904 (w), 836 (w), 809 (w), 778 (w), 757 (w), 744 (w), 727 (w), 655 (w) cm^{-1}. UV/Vis (CH_2Cl_2): λ_{max} (log ε) = 242 (4.79), 297 (4.80), 421 (4.76), 628 (4.71) nm. UV/Vis (50% CH_2Cl_2/hexane): λ_{max} (log ε) = 242 (4.80), 297 (4.81), 417 (4.77), 617 (4.71) nm. ^{1}H NMR (500 MHz, $CDCl_3$): δ_H = 9.87 (d, *J* = 2.0 Hz, 2 H, 4-H), 8.31 (d, *J* = 10.0 Hz, 2 H, 8-H), 8.16 (s, 2 H, 2-H), 8.00 (d, *J* = 10.0 Hz, 2 H, 6-H), 7.75 (d, *J* = 9.0 Hz, 4 H, 2′,6′-H), 7.67 (dd, *J* = 10.0, 10.0 Hz, 2 H, 7-H), 7.18–7.15 (m, 8 H, H_{DCNQ} and 3′,5′-H), 7.12–7.04 (m, 3 H, H_{DCNQ} and NH), 3.94 (s, 6 H, CO_2Me), 3.30 (sept, *J* = 7.0 Hz, 2 H, *i*Pr), 1.45 (d, *J* = 7.0 Hz, 12 H, *i*Pr) ppm. ^{13}C NMR (125 MHz, $CDCl_3$): δ_C = 170.38 (C_{DCNQ}), 164.65 (CO_2Me), 155.01 (C-5), 153.86 [*C*=C(CN)$_2$], 146.21 [*C*=C(CN)$_2$], 145.71 (C-1′), 144.87 (C-8a), 143.78 (C-3a), 143.37 (C-2), 141.73 (C-6), 140.22 (C-4), 136.37 (C-8 or C_{DCNQ}), 136.27 (C-8 or C_{DCNQ}), 134.04 (C_{DCNQ}), 133.24, 132.18 (C-2′,6′), 131.14 (C-7), 128.13 (C-4′), 125.57 (C_{DCNQ}), 125.10 (C_{DCNQ}), 124.47 (C-1), 119.02 (C-3), 118.13 (C-3′,5′), 114.20 (CN ×2), 113.80 (CN), 112.81 (CN), 83.35 [*C*(CN)$_2$], 74.07 [*C*(CN)$_2$], 51.63 (CO_2Me), 39.35 (*i*Pr), 24.46 (*i*Pr) ppm. HRMS (FAB) calcd. for $C_{70}H_{47}N_9O_4^+$ $[M]^+$ 1077.3746, found 1077.3776. $C_{70}H_{47}N_9O_4 \cdot 2/5H_2O$ (1078.18): calcd. C 77.46, H 4.44, N 11.61; found C 77.52, H 4.50, N 11.60.

Compound 19: To a solution of **12** (200 mg, 0.30 mmol) in EtOAc (10 mL) was added TCNE (102 mg, 0.80 mmol). The resulting mixture was refluxed for 6 h under an Ar atmosphere. The solvent was removed under reduced pressure. The residue was purified by column chromatography on silica gel with CH2Cl2/EtOAc (20:1) to give **19** (255 mg, 92%) as red crystals, m.p. 217.0–220.0 °C decomp. (CH_2Cl_2/hexane). IR (KBr disk): $\tilde{\nu}_{max}$ = 2957 (w), 2875 (w), 2221 (m), 1700 (m), 1628 (w), 1600 (m), 1496 (s), 1442 (s), 1418 (s), 1363 (m), 1313 (w), 1280 (w), 1255 (m), 1236 (s), 1213 (s), 1179 (s), 1143 (s), 1087 (w), 1041 (w), 904 (w), 812 (m), 777 (m), 729 (w), 695 (w), 678 (w) cm^{-1}. UV/Vis (CH_2Cl_2): λ_{max} (log ε) = 233 (4.78), 266 (4.77), 299 (4.80), 347 sh (4.55), 403 (4.50), 456 (4.58) nm. UV/Vis (20% CH_2Cl_2/hexane): λ_{max} (log ε) = 233 (4.78), 263 (4.78), 299 (4.80), 347 sh (4.55), 402 (4.53), 449 (4.55) nm. ^{1}H NMR (500 MHz, $CDCl_3$): δ_H = 9.95 (d, *J* = 2.0 Hz, 2 H, 4-H), 9.50 (s, 1 H, NH), 8.61 (d, *J* = 1.5 Hz, 2 H, 4′,5′-H), 8.55 (d, *J* = 10.0 Hz, 2 H, 8-H), 8.27 (s, 2 H, 2-H), 8.14 (d, *J* = 10.0 Hz, 2 H, 6-H), 8.00 (dd, *J* = 10.0, 10.0 Hz, 2 H, 7-H), 7.84 (dd, *J* = 9.0, 1.5 Hz, 2 H, 2′,7′-H), 7.44 (d, *J* = 9.0 Hz, 2 H, 1′,8′-H), 3.89 (s, 6 H, CO_2Me), 3.33 (sept, *J* = 7.0 Hz, 2 H, *i*Pr), 1.44 (d, *J* = 7.0 Hz, 12 H, *i*Pr) ppm. ^{13}C NMR (125 MHz, $CDCl_3$): δ_C = 168.69 (C-3′,6′), 164.43 (CO_2Me), 161.01 [*C*=C(CN)$_2$], 157.03 (C-5), 146.14 (C-8a), 143.39 (C-4a′,4b′), 142.59 (C-2 or 6), 142.47 (C-2 or 6), 141.96 (C-3a), 140.72 (C-4), 137.71 (C-8), 132.47 (C-7), 129.42 (C-2′,7′), 124.70 [*C*=C(CN)$_2$], 123.35 (C-8a′,9a′), 123.22 (C-4′,5′), 119.49 (C-1 or 3), 119.35 (C-1 or 3), 113.67 (CN), 113.46 (CN), 113.16 (CN), 112.99 (C-1′,8′), 111.83 (CN), 84.27 [*C*(CN)$_2$], 81.08 [*C*(CN)$_2$], 51.74 (CO_2Me), 39.49 (*i*Pr), 24.47 (*i*Pr) ppm. HRMS (FAB) calcd. for $C_{58}H_{37}N_9O_4^+$ $[M]^+$ 923.2964, found 923.2978. $C_{58}H_{37}N_9O_4$ (923.97): calcd. C 75.39, H 4.04, N 13.64; found C 75.18, H 4.15, N 13.58.

Compound 20: To a solution of **12** (200 mg, 0.30 mmol) in EtOAc (15 mL) was added TCNE (204 mg, 1.00 mmol). The resulting mixture was refluxed for 12 h under an Ar atmosphere. The solvent was removed under reduced pressure. The residue was purified by column chromatography on silica gel with CH_2Cl_2/EtOAc (10:1) to give **20** (271 mg, 84%) as dark green crystals, m.p. 267.0–273.0 °C (CH_2Cl_2/hexane). IR (KBr disk): $\tilde{\nu}_{max}$ = 2957 (w), 2208 (m), 1698 (m), 1599 (m), 1506 (s), 1442 (s), 1419 (s), 1397 (s), 1380 (m), 1358 (m), 1309 (w), 1270 (w), 1213 (s), 1191 (s), 1141 (w), 1087 (w), 1045 (w), 930 (w), 905 (w), 838 (w), 811 (w), 776 (w), 729 (w), 664 (w), 655 (w) cm^{-1}. UV/Vis (CH_2Cl_2): λ_{max} (log ε) = 241 (4.88), 297 (4.91), 386 (4.73), 637 (4.70) nm. UV/Vis (50% CH_2Cl_2/hexane): λ_{max} (log ε) = 240 (4.87), 297 (4.91), 382 (4.72), 626 (4.69) nm. ^{1}H NMR (500 MHz, $CDCl_3$): δ_H = 9.86 (d, *J* = 2.0 Hz, 2 H, 4-H), 9.16 (s, 1 H, NH), 8.57 (d, *J* = 1.5 Hz, 2 H, 4′,5′-H), 8.35 (d, *J* = 10.0 Hz, 2 H, 8-H), 8.23 (s, 2 H, 2-H), 7.98 (d, *J* = 10.0 Hz, 2 H, 6-H), 7.74 (dd, *J* = 8.5, 1.5 Hz, 2 H, 2′,7′-H), 7.68 (dd, *J* = 10.0, 10.0 Hz, 2 H, 7-H), 7.48 (s, *J* = 8.5 Hz, 2 H, 1′,8′-H), 7.18–7.13 (m, 4 H, H_{DCNQ}), 7.10 (br. s, 4 H, H_{DCNQ}), 3.93 (s, 6 H, CO_2Me), 3.28 (sept, *J* = 7.0 Hz, 2 H, *i*Pr), 1.44 (d, *J* = 7.0 Hz, 12 H, *i*Pr) ppm. ^{13}C NMR (125 MHz, $CDCl_3$): δ_C = 172.23 (C_{DCNQ}), 164.68 (CO_2Me), 155.04 (C-5), 153.75 [*C*=C(CN)$_2$], 146.30 (C_{DCNQ}), 144.85 (C-8a), 143.86 [*C*=C(CN)$_2$], 143.52 (C-2), 142.91 (C-3a), 141.78 (C-6), 140.22 (C-4), 136.35 (C-8 and C_{DCNQ}), 134.09, 133.83 (C_{DCNQ}), 131.29 (C-7), 129.33 (C-2′,7′), 127.73, 125.72, 125.19 (C_{DCNQ}), 124.69 (C_{DCNQ}), 123.54 (C-1), 123.18 (C-4′,5′), 119.04 (C-3), 114.15 (CN ×2), 113.97 (C-1′,8′ and CN), 112.69 (CN), 84.87 [*C*(CN)$_2$], 74.30 [*C*(CN)$_2$], 51.66 (CO_2Me), 39.36 (*i*Pr), 24.46 (*i*Pr) ppm. HRMS (FAB) calcd. for $C_{70}H_{45}N_9O_4^+$ $[M]^+$ 1075.3590, found 1075.3605. $C_{70}H_{45}N_9O_4 \cdot 3/4H_2O$ (1076.16): calcd. C 77.16, H 4.30, N 11.57; found C 77.26, H 4.41, N 11.56.

Compound 21: To a solution of **13** (199 mg, 0.20 mmol) in EtOAc (10 mL) was added TCNE (128 mg, 1.00 mmol). The resulting mixture was refluxed for 6 h under an Ar atmosphere. The solvent was removed under reduced pressure. The residue was purified by column chromatography on silica gel with CH_2Cl_2/EtOAc (10:1) to

give **21** (249 mg, 90%) as red crystals, m.p. 201.0–205.0 °C decomp. (CH_2Cl_2/hexane). IR (KBr disk): $\tilde{\nu}_{max}$ = 2962 (w), 2879 (w), 2221 (m), 1698 (m), 1590 (m), 1496 (s), 1441 (m), 1418 (m), 1363 (w), 1327 (w), 1291 (m), 1240 (w), 1212 (m), 1181 (s), 1134 (w), 1086 (w), 1053 (w), 906 (w), 812 (w), 778 (m), 732 (m), 712 (w), 668 (w) cm^{-1}. UV/Vis (CH_2Cl_2): λ_{max} (log ε) = 264 (4.95), 300 (4.92), 338 sh (4.73), 404 (4.66), 503 (4.86) nm. UV/Vis (20% CH_2Cl_2/hexane): λ_{max} (log ε) = 264 (4.94), 298 (4.91), 338 sh (4.71), 403 (4.64), 488 (4.84) nm. ^1H NMR (500 MHz, $CDCl_3$): δ_H = 10.01 (d, J = 2.0 Hz, 3 H, 4-H), 8.47 (d, J = 10.0 Hz, 3 H, 8-H), 8.29 (s, 3 H, 2-H), 8.17 (d, J = 10.0 Hz, 3 H, 6-H), 8.00 (dd, J = 10.0, 10.0 Hz, 3 H, 7-H), 7.87 (d, J = 9.0 Hz, 6 H, 2′,6′-H), 7.39 (d, J = 9.0 Hz, 6 H, 3′,5′-H), 3.97 (s, 9 H, CO_2Me), 3.36 (sept, J = 7.0 Hz, 3 H, *i*Pr), 1.48 (d, J = 7.0 Hz, 18 H, *i*Pr) ppm. ^{13}C NMR (125 MHz, $CDCl_3$): δ_C = 167.07 [*C*=C(CN)$_2$], 164.31 (CO_2Me), 160.38 [*C*=C(CN)$_2$], 157.31 (C-5), 149.80 (C-1′), 146.24 (C-8a), 142.72 (C-6), 142.45 (C-2), 141.98 (C-3a), 140.91 (C-4), 137.63 (C-8), 132.45 (C-7), 132.16 (C-2′,6′), 128.80 (C-4′), 125.26 (C-3′,5′), 119.70 (C-1), 119.50 (C-3), 113.61 (CN), 112.56 (CN), 112.37 (CN), 111.33 (CN), 86.17 [*C*(CN)$_2$], 80.53 [*C*(CN)$_2$], 51.81 (CO_2Me), 39.53 (*i*Pr), 24.48 (*i*Pr) ppm. HRMS (FAB) calcd. for $C_{87}H_{57}N_{13}O_6^+$ $[M]^+$ 1379.4550, found 1379.4575. $C_{87}H_{57}N_{13}O_6 \cdot 3/4H_2O$ (1380.47): calcd. C 74.96, H 4.23, N 13.06; found C 75.11, H 4.41, N 13.05.

Compound 22: To a solution of **13** (199 mg, 0.20 mmol) in EtOAc (20 mL) was added TCNQ (204 mg, 1.00 mmol). The resulting mixture was refluxed for 24 h under an Ar atmosphere. The solvent was removed under reduced pressure. The residue was purified by column chromatography on silica gel with CH_2Cl_2/EtOAc (10:1) to give **22** (280 mg, 87%) as dark green crystals, m.p. 264.0–267.0 °C decomp. (CH_2Cl_2/hexane). IR (KBr disk): $\tilde{\nu}_{max}$ = 2959 (w), 2209 (m), 1697 (m), 1591 (m), 1503 (s), 1440 (s), 1420 (s), 1383 (m), 1330 (m), 1279 (m), 1212 (s), 1191 (s), 1128 (w), 1086 (w), 1032 (w), 972 (w), 904 (w), 839 (w), 809 (w), 777 (w), 729 (w), 698 (w), 673 (w), 657 (w) cm^{-1}. UV/Vis (CH_2Cl_2): λ_{max} (log ε) = 243 (5.01), 296 (5.05), 394 sh (4.83), 422 (4.89), 628 (4.85) nm. UV/Vis (50% CH_2Cl_2/hexane): λ_{max} (log ε) = 243 (4.99), 296 (5.02), 394 sh (4.83), 419 (4.89), 617 (4.83) nm. ^1H NMR (500 MHz, $CDCl_3$): δ_H = 9.88 (d, J = 1.5 Hz, 3 H, 4-H), 8.28 (d, J = 10.0 Hz, 3 H, 8-H), 8.15 (s, 3 H, 2-H), 8.02 (d, J = 10.0 Hz, 3 H, 6-H), 7.72 (d, J = 8.0 Hz, 6 H, 2′,6′-H), 7.67 (dd, J = 10.0, 10.0 Hz, 1 H, 7-H), 7.19–7.13 (m, 12 H, H_{DCNQ} and 3′,5′-H), 7.07–7.01 (m, 6 H, H_{DCNQ}), 3.96 (s, 9 H, CO_2Me), 3.31 (sept, J = 7.0 Hz, 1 H, *i*Pr), 1.47 (d, J = 7.0 Hz, 18 H, *i*Pr) ppm. ^{13}C NMR (125 MHz, $CDCl_3$): δ_C = 170.23 (C_{DCNQ}), 164.64 (*C*O_2Me), 155.10 (C-5), 153.62 [*C*=C(CN)$_2$], 149.25 (C-1′), 145.13 [*C*=C(CN)$_2$], 144.75 (C-8a), 143.82 (C-3a), 143.05 (C-2), 141.87 (C-6), 140.29 (C-4), 136.37 (C-8), 136.15 (C_{DCNQ}), 133.68 (C_{DCNQ}), 133.25 (C-4′), 131.78 (C-2′,6′), 131.19 (C-7), 131.01, 125.78 (C_{DCNQ}), 125.32 (C_{DCNQ}), 124.84 (C-3′,5′), 124.17 (C-1), 119.13 (C-3), 114.07 (CN), 113.96 (CN), 113.24 (CN), 112.27 (CN), 85.93 [*C*(CN)$_2$], 74.94 [*C*(CN)$_2$], 51.72 (CO_2Me), 39.38 (*i*Pr), 24.48 (*i*Pr) ppm. HRMS (FAB) calcd. for $C_{105}H_{69}N_{13}O_6^+$ $[M]^+$ 1607.5489, found 1607.5481. $C_{105}H_{69}N_{13}O_6 \cdot H_2O$ (1608.76): calcd. C 77.52, H 4.40, N 11.19; found C 77.65, H 4.52, N 11.12.

Supporting Information (see footnote on the first page of this article): Copies of ^1H and ^{13}C NMR, UV/Vis spectra and continuous change in the visible spectra of the reported compounds.

Acknowledgments

This work was partially supported by a Grant-in-Aid for Research from the Ministry of Education, Culture, Sports, Science, and Technology, Japan 22850007 and 25810019 to T. S.

[1] a) J. Kido, Y. Okamoto, *Chem. Rev.* **2002**, *102*, 2357–2368; b) A. C. Grimsdale, K. L. Chan, R. E. Martin, P. G. Jokisz, A. B. Holmes, *Chem. Rev.* **2009**, *109*, 897–1091; c) M. Zhu, J. Zou, X. He, C. Yang, H. Wu, C. Zhong, J. Qin, Y. Cao, *Chem. Mater.* **2012**, *24*, 174–180; d) Y. Zhang, S.-L. Lai, Q.-X. Tong, M.-F. Lo, T.-W. Ng, M.-Y. Chan, Z.-C. Wen, J. He, K.-S. Jeff, X.-L. Tang, W.-M. Liu, C.-C. Ko, P.-F. Wang, C.-S. Lee, *Chem. Mater.* **2012**, *24*, 61–70; e) Y. Liu, S. Chen, J. W. Y. Lam, P. Lu, R. T. K. Kwok, F. Mahtab, H. S. Kwok, B. Z. Tang, *Chem. Mater.* **2011**, *23*, 2536–2544.

[2] a) J. Rivnay, S. C. B. Mannsfeld, C. E. Miller, A. Salleo, M. F. Toney, *Chem. Rev.* **2012**, *112*, 5488–5519; b) S. Feser, K. Meerholz, *Chem. Mater.* **2011**, *23*, 5001–5005.

[3] a) S.-C. Lo, P. L. Burn, *Chem. Rev.* **2007**, *107*, 1097–1116; b) Y.-J. Cheng, S.-H. Yang, C.-S. Hsu, *Chem. Rev.* **2009**, *109*, 5868–5923; c) X. Ren, S. Jiang, M. Cha, G. Zhou, Z.-S. Wang, *Chem. Mater.* **2012**, *24*, 3493–3499; d) W. Z. Yuan, Y. Gong, S. Chen, X. Y. Shen, J. W. Y. Lam, P. Lu, Y. Lu, Z. Wang, R. Hu, N. Xie, H. S. Kwok, Y. Zhang, J. Z. Sun, B. Z. Tang, *Chem. Mater.* **2012**, *24*, 1518–1528; e) Y. Sun, S.-C. Chien, H.-L. Yip, Y. Zhang, K.-S. Chen, D. F. Zeigler, F.-C. Chen, B. Lin, A. K.-Y. Jen, *Chem. Mater.* **2011**, *23*, 5006–5015.

[4] a) X.-D. Zhuang, Y. Chen, B.-X. Li, D.-G. Ma, B. Zhang, Y. Li, *Chem. Mater.* **2010**, *22*, 4455–4461; b) W.-Y. Lee, T. Kurosawa, S.-T. Lin, T. Higashihara, M. Ueda, W.-C. Chen, *Chem. Mater.* **2011**, *23*, 4487–4497; c) Q.-D. Ling, D.-J. Liaw, C. Zhu, D. S.-H. Chan, E.-T. Kang, K.-G. Neoh, *Prog. Polym. Sci.* **2008**, *33*, 917–978; d) K.-L. Wang, Y.-L. Liu, I.-H. Shin, K.-G. Neoh, E.-T. Kang, *J. Polym. Sci., Part A: Polym. Chem.* **2010**, *48*, 5790–5800; e) K.-L. Wang, Y.-L. Liu, J.-W. Lee, K.-G. Neoh, E.-T. Kang, *Macromolecules* **2010**, *43*, 7159–7164.

[5] a) A. Leliege, P. Blanchard, T. Rousseau, J. Roncali, *Org. Lett.* **2011**, *13*, 3098–3101; b) J. Wu, J. Liu, T. Zhou, S. Bo, L. Qiu, Z. Zhen, X. Liu, *RSC Adv.* **2012**, *2*, 1416–1423; c) A. R. Morales, A. Frazer, A. W. Woodward, H.-Y. Ahn-White, A. Fonari, P. Tongwa, T. Timofeeva, K. D. Belfield, *J. Org. Chem.* **2013**, *78*, 1014–1025.

[6] a) S. Kato, F. Diederich, *Chem. Commun.* **2010**, *46*, 1994–2006; b) M. Kivala, F. Diederich, *Acc. Chem. Res.* **2009**, *42*, 235–248; c) M. Kivala, T. Stanoeva, T. Michinobu, B. Frank, G. Gescheidt, F. Diederich, *Chem. Eur. J.* **2008**, *14*, 7638–7647; d) B. B. Frank, B. C. Blanco, S. Jakob, F. Ferroni, S. Pieraccini, A. Ferrarini, C. Boudon, J.-P. Gisselbrecht, P. Seiler, G. P. Spada, F. Diederich, *Chem. Eur. J.* **2009**, *15*, 9005–9016; e) P. Fesser, C. Iacovita, C. Wäckerlin, S. Vijayaraghavan, N. Ballav, K. Howes, J.-P. Gisselbrecht, M. Crobu, C. Boudon, M. Stchr, T. A. Jung, F. Diederich, *Chem. Eur. J.* **2011**, *17*, 5246–5250; f) B. Breiten, Y.-L. Wu, P. D. Jarowski, J.-P. Gisselbrecht, C. Boudon, M. Griesser, C. Onitsch, G. Gescheidt, W. B. Schweizer, N. Langer, C. Lennartz, F. Diederich, *Chem. Sci.* **2011**, *2*, 88–93; g) A. R. Lacy, A. Vogt, C. Boudon, J.-P. Gisselbrecht, W. B. Schweizer, F. Diederich, *Eur. J. Org. Chem.* **2013**, 869–879; h) B. H. Tchitchanov, M. Chiu, M. Jordan, M. Kivala, W. B. Schweizer, F. Diederich, *Eur. J. Org. Chem.* **2013**, 3729–3740.

[7] a) T. Michinobu, *Chem. Soc. Rev.* **2011**, *40*, 2306–2316; b) Y. Yuan, T. Michinobu, *J. Polym. Sci., Part A: Polym. Chem.* **2011**, *49*, 225–233; c) H. Fujita, K. Tsuboi, T. Michinobu, *Macromol. Chem. Phys.* **2011**, *212*, 1758–1766; d) Y. Washino, T. Michinobu, *Macromol. Rapid Commun.* **2011**, *32*, 644–648; e) Y. Li, M. Ashizawa, S. Uchida, T. Michinobu, *Macromol. Rapid Commun.* **2011**, *32*, 1804–1808; f) T. Michinobu, C. Seo, K. Noguchi, T. Mori, *Polym. Chem.* **2012**, *3*, 1427–1435; g) Y. Li, M. Ashizawa, S. Uchida, T. Michinobu, *Polym. Chem.* **2012**, *3*, 1996–2005; h) T. Michinobu, *J. Synth. Org. Chem. Jpn.* **2013**, *71*, 149–157.

[8] a) T. Shoji, S. Ito, K. Toyota, M. Yasunami, N. Morita, *Chem. Eur. J.* **2008**, *14*, 8398–8408; b) T. Shoji, S. Ito, K. Toyota, T. Iwamoto, M. Yasunami, N. Morita, *Eur. J. Org. Chem.* **2009**, 4316–4324; c) T. Shoji, M. Maruyama, S. Ito, N. Morita, *Bull.*

Chem. Soc. Jpn. **2012**, *85*, 761–773; d) T. Shoji, S. Ito, T. Okujima, N. Morita, *Org. Biomol. Chem.* **2012**, *10*, 8308–8313; e) T. Shoji, S. Ito, T. Okujima, N. Morita, *Chem. Eur. J.* **2013**, *19*, 5721–5730.

[9] a) T. Shoji, J. Higashi, S. Ito, T. Okujima, M. Yasunami, N. Morita, *Chem. Eur. J.* **2011**, *17*, 5116–5129; b) T. Shoji, J. Higashi, S. Ito, T. Okujima, M. Yasunami, N. Morita, *Org. Biomol. Chem.* **2012**, *10*, 2431–2438.

[10] T. Shoji, S. Ito, T. Okujima, N. Morita, *Eur. J. Org. Chem.* **2011**, 5134–5140.

[11] J.-P. Corbet, G. Mignani, *Chem. Rev.* **2006**, *106*, 2651–2710.

[12] R. Boothe, C. Dial, R. Conaway, R. M. Pagni, G. W. Kabalka, *Tetrahedron Lett.* **1986**, *27*, 2207–2210.

[13] a) S. M. Hubig, W. Jung, J. K. Kochi, *J. Org. Chem.* **1994**, *59*, 6233–6244; b) T. Mukaiyama, H. Kitagawa, J. Matsuo, *Tetrahedron Lett.* **2000**, *41*, 9383–9386.

[14] a) K. J. Edgar, S. N. Falling, *J. Org. Chem.* **1990**, *55*, 5287–5291; b) G. A. Olah, G. Q. W. Sandford, P. G. K. Surya, *J. Org. Chem.* **1993**, *58*, 3194–3195; c) M. C. Carreno, J. L. G. Ruano, A. G. S. Miguel, A. Urbano, *Tetrahedron Lett.* **1996**, *37*, 4081–4084; d) A. S. Castanet, F. Colobert, P. E. Broutin, *Tetrahedron Lett.* **2002**, *43*, 5047–5048.

[15] T. Yamamoto, K. Toyota, N. Morita, *Tetrahedron Lett.* **2010**, *51*, 1364–1366.

[16] S. Kajigaeshi, T. Kakinami, H. Yamasaki, S. Fujisaki, T. Okamoto, *Bull. Chem. Soc. Jpn.* **1988**, *61*, 600–602.

[17] a) Z.-H. Zhao, H. Jin, Y.-X. Zhang, Z. Shen, D.-C. Zou, X.-H. Fan, *Macromolecules* **2011**, *44*, 1405–1413; b) Y. Wu, H. Guo, T. D. James, J. Zhao, *J. Org. Chem.* **2011**, *76*, 5685–5695.

[18] Y. Shirota, T. Kobata, N. Noma, *Chem. Lett.* **1989**, *18*, 1145–1148.

[19] T. Shoji, E. Shimomura, M. Maruyama, S. Ito, T. Okujima, N. Morita, *Eur. J. Org. Chem.* **2013**, 957–964.

[20] a) K. Sonogashira, Y. Tohda, N. Hagihara, *Tetrahedron Lett.* **1975**, *16*, 4467–4470; b) S. Takahashi, Y. Kuroyama, K. Sonogashira, N. Hagihara, *Synthesis* **1980**, 627–630; c) K. Sonogashira, *Coupling reactions between sp^2 and sp carbon centers*, in: *Comprehensive Organic Synthesis* vol. 3 (Eds.: B. M. Trost, I. Fleming), Pergamon, Oxford, UK, **1991**, chapter 2.4, p. 521–549; d) K. Sonogashira, *Cross-coupling reactions to sp carbon atoms*, in: *Metal-Catalyzed Cross-Coupling Reactions* (Eds.: F. Diederich, P. J. Stang), Wiley-VCH, Weinheim, Germany, **1998**, chapter 5, p. 203–229.

[21] M. Jordan, M. Kivala, C. Boudon, J.-P. Gisselbrecht, W. B. Schweizer, P. Seiler, F. Diederich, *Chem. Asian J.* **2011**, *6*, 396–401.

[22] M. Kivala, C. Boudon, J.-P. Gisselbrecht, P. Seiler, M. Gross, F. Diederich, *Chem. Commun.* **2007**, 4731–4733.

[23] a) P. Suppan, N. Ghoneim, *Solvatochromism*, Royal Society of Chemistry, Cambridge, UK, **1997**; b) P. Suppan, *J. Photochem. Photobiol. A: Chem.* **1990**, *50*, 293–330; c) C. Reichardt, *Solvent and Solvent Effects in Organic Chemistry*, Wiley-VCH, New York, **2004**.

[24] The B3LYP/6-31G(d) time-dependence density functional calculations were performed with Spartan′10, Wavefunction, Irvine, CA.

[25] a) S. Ito, N. Morita, *Eur. J. Org. Chem.* **2009**, 4567–4579; b) S. Ito, T. Shoji, N. Morita, *Synlett* **2011**, *16*, 2279–2298.

Received: July 7, 2013
Published Online: October 9, 2013

